nature reviews bioengineering

https://doi.org/10.1038/s44222-024-00241-x

Review article

Check for updates

Bioengineering embryo models

Xufeng Xue[1], Yue Liu[1] & Jianping Fu[1,2,3]

Abstract

Stem cell-based embryo models, which recapitulate symmetry breaking, pattern formation and tissue morphogenesis during early development, provide promising experimental tools to study the development of mammalian species, including humans. Despite considerable progress in embryo modelling using cultured stem cells, generating embryo models with high fidelity, efficiency, controllability, and in vivo-like cellular organization and tissue architecture remains challenging. This is largely due to intrinsic variabilities in self-organization and differentiation of mammalian stem cells in uncontrolled culture environments. In this Review, we argue that bioengineering tools, which are powerful for controlling topological boundaries and dynamic chemical and mechanical signals, can efficiently guide symmetry breaking, pattern formation, tissue morphogenesis and tissue–tissue interactions. We discuss pattern formation and morphogenesis during embryonic development and examine different embryo models to highlight the importance of bioengineering strategies in developing models with improved efficiency, reproducibility, controllability, complexity and in vivo relevance.

Sections

Introduction

Pattern formation

Tissue morphogenesis

Synthetic biology for embryo models

Outlook

[1]Department of Mechanical Engineering, University of Michigan, Ann Arbor, MI, USA. [2]Department of Biomedical Engineering, University of Michigan, Ann Arbor, MI, USA. [3]Department of Cell & Developmental Biology, University of Michigan Medical School, Ann Arbor, MI, USA. e-mail: jpfu@umich.edu

Key points

- Stem cell-based embryo models can recapitulate essential developmental processes such as tissue patterning and morphogenetic events from pre-implantation to early organogenesis.
- Bioengineering strategies enable control of tissue geometrical boundaries and interactions, chemical gradients, and extracellular matrix signals to improve the efficiency and fidelity of stem cell-based embryo modelling.
- Synthetic biology approaches can provide programmable cellular complexity, architecture and function in bioengineered embryo models.
- Bioengineered embryo models with improved efficiency, controllability, reproducibility and scalability hold promise for fundamental and translational applications.

Introduction

During development, patterned multicellular structures with stereotypical 3D tissue architecture emerge from a single fertilized egg. Mammalian development involves coordinated developmental processes, including pattern formation, tissue morphogenesis, cell differentiation and growth[1]. Pattern formation establishes body axes in mammalian embryos, including anterior (head) to posterior (tail) (A–P) and dorsal (back) to ventral (belly) (D–V) axes. Mammalian embryos undergo substantial morphological changes in form, termed morphogenesis, to achieve complex tissue and organ anatomies. Mammalian development also involves cell differentiation, through which specialized cell types with tissue-specific or organ-specific functions would arise, and tissue growth. These developmental processes are intricately linked during dynamic, progressive development. Precisely how the mammalian embryo develops from a fertilized egg through these coordinated developmental processes remains one of the most fundamental questions in biology with enormous biomedical implications.

Recent advances in stem cell biology, developmental biology and bioengineering have fostered the emergence of an exciting interdisciplinary field termed stem cell-based embryo models[2–5]. This field aims to apply developmental biology principles to create embryo models using mammalian pluripotent and extra-embryonic stem cells in vitro. When differentiated in vitro, these stem cells largely follow the natural developmental programmes of their in vivo counterparts[6]. Since the mid-2010s, numerous studies have showcased the intrinsic self-organizing properties of these cells to differentiate and self-assemble into embryonic-like or extra-embryonic-like structures in vitro[7,8]. These models can recapitulate major developmental processes such as tissue patterning and morphogenetic events during pre-implantation, gastrulation, neurulation and somitogenesis[3,4,9] (Table 1). Nonetheless, future applications of stem cell-based embryo models hinge on the premise that these models can serve as useful experimental tools to disentangle the genetic, molecular and cellular events involved in human embryogenesis[3,10,11] (Box 1).

Despite considerable excitement and success, embryo models fail to efficiently and faithfully recapitulate tissue patterning or morphogenetic events occurring in natural embryonic development, which hinders their broad application. This is largely because approaches for embryo modelling rely on the spontaneous differentiation and self-organization of mammalian stem cells and their progenies in uncontrolled culture environments. Thus, their development is influenced by stochastic genetic noises (which arise from stochastic variations in the synthesis and degradation of mRNA and proteins[12]) or random cellular interactions with the local culture microenvironment[13]. So far, a variety of mammalian stem cells, including pluripotent stem (PS) cells and stem cells of extra-embryonic lineages, such as trophoblast stem cells (TSCs)[14,15] and extra-embryonic endoderm cells (XENs)[16], have been used to generate embryo models. However, culture conditions of these stem cells have not yet been standardized and human extra-embryonic stem cells remain to be fully established. Moreover, human PS (hPS) cells generated using different culture protocols have distinct pluripotency states with varied differentiation potentials[17]. The variability of mammalian stem cells further complicates robust development and limits the usefulness of embryo models. In this Review, we highlight how bioengineering tools can be used to improve the efficiency and fidelity of embryo models.

Pattern formation

In development, pattern formation is the process by which cellular activity is organized both spatially and temporally such that a well-ordered tissue structure develops[18]. Pattern formation can be either self-organized[19] or guided by external cues[20]; the former involves patterning of cell fates through spontaneous cell–cell interactions amongst a seemingly homogeneous cell population[19]. One such system, proposed by Turing, is based on the reaction–diffusion model, in which stable patterns emerge via cell–cell interactions through diffusion of activator–inhibitor pairs[21]. Turing's reaction–diffusion model has successfully explained pattern formation in various in vivo (such as hair follicle patterning[22]) and in vitro (such as two-dimensional or 2D gastrulation models[23]) systems. The initial and boundary conditions of morphogenetic fields of pattern formation are critical for self-organized pattern formation[19]. Thus, bioengineering approaches that can control the initial cell number and geometries of cell colonies have been used to generate robust embryo models whose developments rely on self-organized pattern formation[24,25].

For external cue-guided pattern formation, spatially patterned cell fates are instructed by external signals, such as diffusible molecules, including both morphogens and their antagonists, secreted from adjacent preformed tissues that function as signalling centres. External cue-guided pattern formation can be explained by the positional information theory proposed by Wolpert[26]. This theory proposes that external morphogens provide positional values as in a coordinate system for cell fate decisions[26]. Bioengineering approaches, such as co-culture systems and microfluidic devices, can be used to control paracrine signals and to generate dynamic morphogen gradients, respectively[13,27], which serve as external cues to guide pattern formation in embryo models[28–31].

Even though pattern formation in vivo often involves both self-organized cell–cell interactions and external cue-guided spatial fate patterning[32], there are embryonic development events in which each of these mechanisms has a specific role. In this section, we first discuss three such events, their corresponding embryo models, and the bioengineering approaches in recapitulating pattern formation in these models: (1) specification of trophectoderm, hypoblast (primitive endoderm or PrE in mice) and epiblast (EPI) during blastocyst formation through self-organized pattern formation; (2) A–P symmetry breaking in the EPI at the onset of gastrulation guided by extra-embryonic tissues; and (3) neural tube patterning via morphogen gradients.

Table 1 | Selected stem cell-based embryo models

Model name	Starting cell population	Approach	Developmental events modelled	Limitations	Refs.
Mouse embryo models					
Blastoid	mESC+mTSC; mEPSC; mEPSC+mTSC	Cell aggregation in microwell	Blastocyst formation; TE, EPI and PrE lineage segregation	Underdeveloped PrE; limited developmental potential	50–52
ETS embryoid	mESC+mTSC	Cell aggregation in microwell	Post-implantation ExE and EPI compartment formation; EPI patterning	Low efficiency (~20%); lack of VE	67
ETX embryoid	mESC+mTSC+mXEN; mESC+mTSC+i*Gata4* mESC	Cell aggregation in microwell	Post-implantation ExE, VE and EPI compartment formation; AVE and A–P axis formation; initiation of EMT and gastrulation	Low efficiency (15–40%)	68,69,194
Advanced ETX embryoid	mESC+mTSC+i*Gata4* mESC; mESC+i*Cdx2* mESC+i*Gata4* mESC	Cell aggregation in microwell; ex utero roller culture system	Post-implantation development up to neurulation and early organogenesis	Low efficiency (less than 1%); structural defects in organ primordia	70–72
EpiTS embryoid	mESC+mTSC	Assembloid	Post-implantation EPI symmetry breaking and initiation of EMT	Lack of in vivo-like tissue morphology	74
Peri-gastrulation assembloid	mESC+BMP4-treated mESC	Assembloid	Post-implantation A–P and D–V patterning of three-germ layer lineages	Lack of forebrain; limited morphogenesis; structural defects in organ primordia	28
Gastruloid	mESC	Cell aggregation in microwell	Post-implantation A–P patterning of germ layer lineages; axial elongation	Limited morphogenetic events	142
Gastruloid with ECM	mESC	Cell aggregation in microwell; Matrigel embedding	Post-implantation A–P patterning of germ layer lineages; axial elongation; somite formation	Low efficiency (~50%)	135
D–V patterned neural cyst	mESC	Matrigel embedding; synthetic hydrogel	Spinal cord D–V patterning	Low efficiency (~6%); lack of control of biochemical gradients	95,97
Trunk-like structure	mESC	Cell aggregation in microwell; Matrigel embedding	Post-implantation A–P patterning of germ layer lineages; axial elongation; somite and neural tube co-development	Lack of control of biochemical gradients	137
Human embryo models					
Blastoid	Naive hPSC; hEPSC; fibroblast reprogramming intermediate	Cell aggregation in microwell	Blastocyst formation; TE, EPI and PrE lineage segregation	Underdeveloped PrE; limited developmental potential	24,53–57,81
PASE	Primed hPSC	Microfluidics	Post-implantation amnion–EPI patterning; PGC development; initiation of EMT and gastrulation	Lack of A–P patterning in EPI	29,79
heX embryoid	Primed hPSC+i*GATA6* hPSC	Co-culture	Post-implantation amnion–EPI patterning; bilaminar disc; A–P patterning of EPI; yolk sac formation; haematopoiesis	Unclear identity of i*GATA6* hPSCs; limited development of embryonic germ layers	82
Bilaminoid	Naive hPSC+i*GATA6* hPSC	Cell aggregation in microwell	Post-implantation amnion–EPI patterning; bilaminar disc; A–P patterning of EPI	Low efficiency (20–40%)	87
Extra-embryoid	hPSC with intermediate pluripotency	Cell aggregation in microwell	EPI and hypoblast segregation; amnion–EPI patterning; A–P patterning of EPI	Low A–P patterning efficiency (~8%)	85
Inducible embryoid	Naive hPSC+i*GATA6*–*SOX17* hPSC+i*GATA3*–*TFAP2C* hPSC	Cell aggregation in microwell	Post-implantation amnion–EPI patterning; PGC specification	Low efficiency (~20%); lack of yolk sac-like structure	86
Peri-gastruloid	hEPSC	Cell aggregation in microwell	Bilaminar disc; amnion–EPI patterning; A–P patterning of EPI; initiation of EMT and gastrulation; PGC specification; yolk sac formation	Unclear morphogenetic events; unclear A–P patterning efficiency; lack of trophoblast cells	83
SEM	Naive hPSC+chemically induced PrE-like and trophoblast-like cells	Cell aggregation in microwell; ex utero roller culture system	Bilaminar disc; amnion–EPI patterning; A–P patterning of EPI; PGC specification; yolk sac formation; development of ExE and TE lineage	Low efficiency (~1%)	84
2D gastrulation model	Primed hPSC	Micropattern	Patterning of three-germ layer lineages	Limited morphogenetic events	25
2D gastrulation model on soft gel	Primed hPSC	Micropattern; synthetic hydrogel	EMT and mesoderm ingression	Limited germ layer patterning	148
Gastruloid	Primed hPSC	Cell aggregation in microwell	A–P patterning of germ layer lineages; axial elongation	Limited morphogenetic events	143

Table 1 (continued) | Selected stem cell-based embryo models

Mouse embryo models					
Model name	**Starting cell population**	**Approach**	**Developmental events modelled**	**Limitations**	**Refs.**
Human embryo models (continued)					
2D neural rosette	Primed hPSC	Micropattern	Neural tube morphology	Limited cell fate patterning or morphogenetic events	191,195
2D ectoderm model	Primed hPSC	Micropattern	NP and NPB patterning	Limited morphogenetic events; lack of NNE	109
	Primed hPSC	Micropattern	Ectoderm patterning	Limited morphogenetic events	163
	Primed hPSC	Micropattern	Ectoderm patterning; neural cyst formation	Limited morphogenetic events	164
Cranial neurulation model	Primed hPSC	Micropattern; Matrigel embedding	Cranial neural tube folding and closure	Lack of A–P or D–V axis	136
Spinal cord neurulation model	Primed hPSC	Cell aggregation in microwell	Spinal cord neural tube folding and closure	Heterogeneity; lack of D–V axis	165
D–V patterned neural cyst	Primed hPSC	Matrigel embedding	Spinal cord D–V patterning	Low efficiency (~30%); lack of control of biochemical gradients	96
A–P patterned neural tube model	Primed hPSC	Microfluidics	Brain region A–P patterning	Lack of 3D tubular morphology; lack of D–V axis	30
μNTLS	Primed hPSC	Microfluidics	Neural tube A–P and D–V patterning	Lack of neural tube folding morphogenesis	31
Somitoid	Primed hPSC	2D culture of spheroids	Somitogenesis	Lack of sequential formation and A–P patterning of somites	174
Segmentoid	Primed hPSC	Cell aggregation in microwell; Matrigel embedding	Axial elongation; A–P patterning; somitogenesis	Lack of control of biochemical gradients	174
Axioloid	Primed hPSC	Cell aggregation in microwell; Matrigel embedding	Axial elongation; A–P patterning; somitogenesis	Lack of control of biochemical gradients	175
μSDM	Primed hPSC	Microfluidics; Matrigel embedding	Somitogenesis	Lack of sequential formation and A–P patterning of somites	176
Trunk-like structure	Primed hPSC	Cell aggregation in microwell; Matrigel embedding	Axial elongation; A–P patterning; somite and neural tube co-development	Lack of control of biochemical gradients	177

A–P, anterior to posterior; D–V, dorsal to ventral; ECM, extracellular matrix; EMT, epithelial–mesenchymal transition. **Embryo model names:** ETS embryoid, ES cell-derived, TSC-derived embryo model; ETX embryoid, ES cell-derived, TSC-derived, XEN-derived embryo model; PASE, post-implantation amniotic sac embryoid; SEM, post-implantation stem cell-based embryo model; μNTLS, microfluidic neural tube-like structure; μSDM, microfluidic somite development model. **Cell lineages:** AVE, anterior visceral endoderm; EPI, epiblast; ExE, extra-embryonic ectoderm; NNE, non-neural ectoderm; NP, neural plate; NPB, neural plate border; PGC, primordial germ cell; PrE, primitive endoderm; TE, trophectoderm; VE, visceral endoderm. **Stem cells:** (mouse) i*Cdx2* mESC, mESCs transiently expressing *Cdx2*; i*Gata4* mESC, mESCs transiently expressing *Gata4*; mEPSC, mouse extended/expanded potential stem cell; mESC, mouse embryonic stem cell; mTSC, mouse trophoblast stem cell; mXEN, mouse extra-embryonic endoderm stem cell. (Human) hEPSC, human extended/expanded potential stem cell; hPSC, human pluripotent stem cell; i*GATA3–TFAP2C* hPSC, hPSCs transiently expressing *GATA3* and *TFAP2C*; i*GATA6* hPSC, hPSCs transiently expressing *GATA6*; i*GATA6–SOX17* hPSC, hPSCs transiently expressing *GATA6* and *SOX17*.

Pattern formation in vivo and in embryo models

Blastocyst formation and modelling through self-organized pattern formation. The first major symmetry-breaking event in mammalian development takes place during blastocyst formation, whereby cells of the morula undergo a series of cell-fate decision events[33,34]. The blastocyst is composed of trophectoderm surrounding the blastocoel and inner cell mass (ICM) (Fig. 1a). After implantation, the trophectoderm contributes to placental development. Within the blastocyst, the ICM differentiates into two distinct cell lineages: EPI, forming the embryo proper, and hypoblast (Fig. 1a).

Lineage segregations during blastocyst formation have mainly been studied in mouse embryos. Segregation between trophectoderm and ICM cells occurs first. At the eight-cell stage, driven by cortical tension, the mouse embryo becomes compacted, and each individual cell acquires an apical domain[35] (Fig. 1a). As mouse morula cells divide, cells in the outer layers inherit apical components and become polarized, whereas those in inner layers become apolar[36] (Fig. 1a). The distinct polarity status leads to differential Hippo signalling and subsequent differential expression of trophectoderm-related and EPI-related transcription factors in the outer and inner cells of the mouse morula, respectively[37,38]. Thus, embryo geometry, coupled with cortical tension, cell position and division pattern, defines the polar-to-apolar cell ratio and therefore trophectoderm and ICM lineage allocation[35,39–41] (Fig. 1a). After this lineage bifurcation, transmembrane pumps in trophectoderm cells pump fluids into the extracellular space, resulting in the formation of small fluid-filled cavities[42]. These cavities coalesce into a single large cavity, the blastocoel, due to pressure imbalance[43]. After blastocoel formation, ICM cells become segregated into EPI

and PrE[33,34]. This process is regulated by heterogeneous FGF signals in the ICM, with EPI precursors secreting FGF ligands to drive PrE fate specification in neighbouring cells[44] (Fig. 1a). Thus, PrE and EPI cells initially form a 'salt-and-pepper' pattern, before cell sorting to establish a well-delineated spatial pattern, with the PrE layer lining the blastocoel and EPI surrounded by PrE and trophectoderm[45].

However, the molecular mechanisms underlying human hypoblast development remain elusive. Earlier studies have shown that FGF inhibition does not substantially influence hypoblast induction in human blastocysts[46,47]. Nevertheless, recent reports suggest that FGF inhibition could suppress hypoblast or hypoblast-like cell specification of human blastocysts or from naive hPS cells, respectively[48,49]. Thus, more investigation is needed to reconcile these discrepancies and fully elucidate the role of FGF signalling in human hypoblast specification.

Stem cell-based models of blastocysts, or blastoids, were first generated using mouse stem cells[50–52] followed by human blastoids developed from human stem cells[24,53–57] (Table 1 and Fig. 1b). Blastoids resemble blastocysts in terms of morphology, transcriptome and lineage composition. Naive hPS cells are often the starting cell population of choice in developing human blastoids owing to their embryonic and extra-embryonic lineage potency[24,54–56]. Regardless of the initial cell types being used, human blastoid protocols commonly involve seeding and aggregating hPS cells in confining microwell plates to initiate and promote self-organized tissue patterning[24,53–57]. Here, the initial cell number in each cell aggregate, dictated by cell seeding density, is an important parameter for blastoid formation[24,54,55]. For example, low cell numbers often lead to the formation of trophoblast spheroids lacking ICM-like cells[54]. After initial cell aggregate formation, cell clusters are then exposed to ERK, ROCK and NODAL inhibitors to induce trophectoderm lineage differentiation[24,54–56]. Similar to the in vivo process, the outer and inner cells in human blastoids acquire differential polarity status and Hippo signalling activity[24,54–56]. Notably, inhibition of Hippo signalling promotes trophectoderm differentiation and increases the efficiency of human blastoid generation[24,56]. Although hypoblast-like cells are present in human blastoids, they are not as organized as their in vivo counterpart and their behaviour and function remain to be fully characterized.

Human blastoids can be generated with high efficiency (~80%) and in large quantities, thereby offering a useful tool to study human pre-implantation and peri-implantation development. For example, co-culturing human blastoids with endometrial epithelial cells and stromal cells[24,56,58] reveals that maturation of trophectoderm cells and their interaction with endometrial epithelial cells are both regulated by signals emanated from EPI-like cells[24]. Endometrial stromal cells also seems to promote the progression of human blastoids into early peri-implantation stages[56].

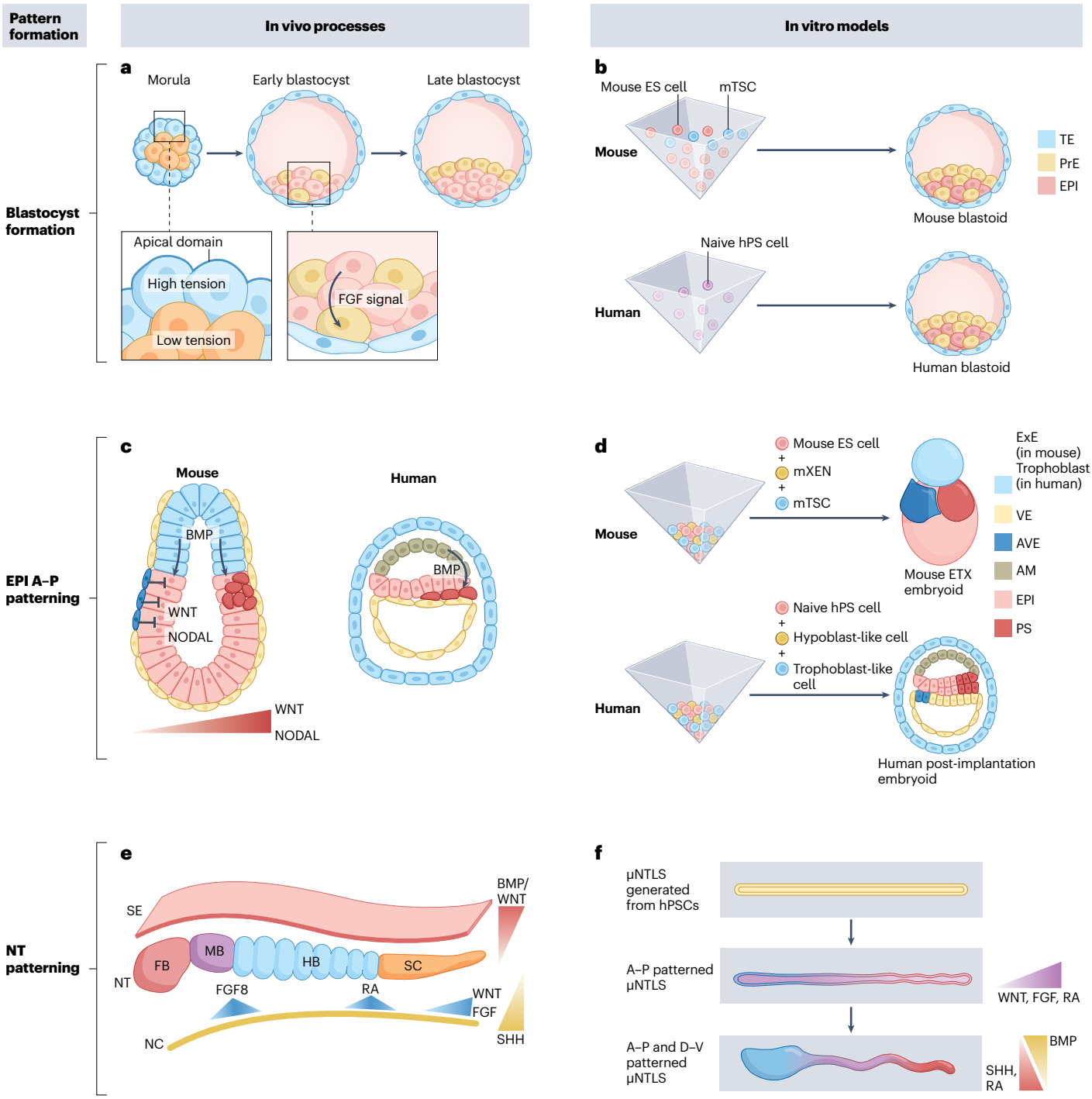
Epiblast symmetry breaking during peri-gastrulation development and its modelling. After implantation, the next milestone of mammalian development is gastrulation, through which the single layer of pluripotent EPI cells transforms into a multilayered and multidimensional structure with fully defined body axes. Mammalian gastrulation has been mainly studied in mouse embryos, revealing the role of extra-embryonic tissues in inducing symmetry breaking of the EPI and establishing the A–P axis at the onset of gastrulation[33]. Specifically, in pre-gastrulation mouse egg cylinder, the EPI is surrounded by the extra-embryonic ectoderm (ExE) derived from trophectoderm and visceral endoderm derived from PrE. Regionalized BMP signals from the ExE leads to the formation of a distal visceral endoderm[59,60], which in turn migrates towards one side of the embryo and specifies into anterior visceral endoderm (AVE), thereby marking the future anterior domain of mouse embryos[61] (Fig. 1c). The AVE secrets WNT, NODAL and BMP antagonists, shielding anterior EPI from posteriorization and thus restricting the primitive streak formation and gastrulation to posterior EPI[62,63] (Fig. 1c).

In contrast to the cup shape of the pre-gastrulation mouse EPI, pre-gastrulation human EPI exhibits a disc-like morphology, and it is juxtaposed with the dorsal amniotic ectoderm and ventral hypoblast[64] (Fig. 1c). How the amniotic ectoderm and hypoblast regulate symmetry breaking and the A–P axis formation in the EPI during human gastrulation remains unclear. In vitro cultures of human embryos have revealed that a portion of hypoblast cells at the putative anterior region expresses BMP, WNT and NODAL antagonists[65,66], similar to the mouse AVE. Nonetheless, whether these cells act as the anterior signalling centre to induce symmetry breaking and establish the A–P axis in the human EPI remains to be elucidated.

Stem cell-based embryo models that recapitulate symmetry breaking and the formation of A–P axis in the EPI offer promising tools to study these developmental events and the underlying genetic, molecular and cellular mechanisms. For example, peri-gastrulation mouse embryo models have been generated by aggregating mouse embryonic stem (ES) cells and mouse TSCs in 3D Matrigel culture[67] (Table 1). Through spontaneous self-organization, some cell aggregates formed organized egg cylinder-like structures, termed the ES cell-derived and TSC-derived embryo model or ETS model[67]. This model comprises mouse ES cell-derived pseudostratified EPI-like epithelium

Box 1 | Applications of embryo models

Stem cell-based embryo models provide an accessible and experimentally tractable method to study mammalian development. Together with genome editing, live-cell imaging and multiomics, stem cell-based embryo models can elucidate molecular and cellular mechanisms in mammalian development. For example, owing to its controllability and compatibility with live-cell imaging, the microfluidic post-implantation amniotic sac embryoid model has been used to unveil a human-specific role of amniotic cells in triggering gastrulation-like events[29]. Pre-implantation embryo models, such as blastoids, have highlighted the role of embryonic and extra-embryonic tissue interactions and could serve to study pregnancy loss arising from corresponding defects. A co-culture system of human blastoids with endometrial organoids has been used to study human implantation and its failure[58]. When combined with patient-derived human pluripotent stem cells and genome-editing technologies, human embryo models could provide new insights into other pathological conditions; for example, models of human neural development have identified the roles of autism risk genes in early human neural development[211] or the embryonic origin of late-onset neurodegenerative diseases such as Huntington disease[164]. By improving efficiency, reproducibility and scalability, embryo models could be used in high-throughput teratogenicity and drug screens. Overall, these models hold promise for advancing fundamental research in developmental and reproductive biology as well as in biomedical applications for the prevention and treatment of pregnancy loss, birth defects and developmental disorders.



juxtaposed with mouse TSC-derived ExE-like cells[67]. Despite lacking visceral endoderm-related lineages, some ETS embryo models could undergo symmetry breaking and give rise to regionalized mesoderm tissues[67]. The mechanism behind this process is unclear, likely due to genetic noises or random cellular interactions with local culture microenvironments. Follow-up studies incorporated mouse XENs (in vitro counterpart of PrE) into ETS, resulting in a more complete peri-implantation mouse embryo model, termed ETX (ES cell-derived, TSC-derived, XEN-derived embryo models)[68,69] (Table 1 and Fig. 1d). These models undergo A–P patterning, evidenced by AVE-like cells expressing signalling antagonists and graded expression of NODAL in posterior EPI-like cells[68,69]. ETX embryo models further exhibited cellular features of gastrulation, including epithelial–mesenchymal transition (EMT) of the EPI and formation of mesoderm and endoderm lineages[68,69]. Both ETS and ETX embryo models have low efficiencies (20–30%) due to random, uncontrolled interactions between

Fig. 1 | Pattern formation in vivo and in embryo models. In vivo process and in vitro modelling of blastocyst formation, epiblast symmetry breaking at the onset of gastrulation and neural tube regional patterning. **a**, Formation of mouse and human blastocysts as a self-organized pattern formation process, involving two rounds of cell lineage specification. The first leads to lineage segregation between trophectoderm and inner cell mass. Inner cell mass cells then become segregated into epiblast (EPI) and primitive endoderm (PrE; or hypoblast in humans), a process likely regulated by FGF signalling. **b**, Aggregation and self-organization of mouse or human stem cells leads to the formation of mouse or human blastoids, respectively[24,50–57]. **c**, After blastocyst implantation, the mouse embryo develops into an elongated structure with a cup-shaped EPI juxtaposed to the extra-embryonic ectoderm (ExE), surrounded by the visceral endoderm. By contrast, post-implantation human EPI exhibits a disc-like morphology, and is juxtaposed with amnion and hypoblast. Gastrulation is initiated in posterior EPI. Symmetry breaking and anterior–posterior (A–P) patterning of mouse EPI is guided by extra-embryonic tissues. Similar mechanisms might be conserved in human gastrulation. **d**, Aggregation of mouse or human embryonic and extra-embryonic cells leads to mouse or human peri-gastrulation embryo models, respectively, recapitulating embryo morphology and A–P patterning of the EPI[68,84]. **e**, Neural tube patterning via external morphogen gradients. A–P patterning of the neural tube is mainly governed by WNT, retinoic acid and FGF signal gradients. Dorsal–ventral (D–V) patterning of neural tubes is mediated by BMP/WNT and sonic hedgehog (SHH) gradients secreted by surface ectoderm and notochord, respectively. **f**, An A–P and D–V patterned neural tube model is achieved by exposing human pluripotent stem (hPS) cell-derived tubular structures to stepwise orthogonal morphogen gradients[31]. AM, amnion; AVE, anterior visceral endoderm; ES cell, embryonic stem cell; ETX embryoid, ES cell-derived, TSC-derived, XEN cell-derived embryo model; FB, forebrain; HB, hindbrain; MB, midbrain; mTSC, mouse trophoblast stem cell; mXEN, mouse extra-embryonic endoderm stem cell; NC, notochord; NT, neural tube; PS, primitive streak; RA, retinoic acid; SC, spinal cord; SE, surface ectoderm; TE, trophectoderm; VE, visceral endoderm; μNTLS, microfluidic neural tube-like structure.

embryonic and extra-embryonic cells[67–69]. Notably, the ETX model could even reveal aspects of post-gastrulation events[70–72] (Table 1). When cultured in an ex utero mouse embryo roller culture system under optimized medium conditions[73], ETX embryo models develop structures mimicking the neural tube, heart, gut tube, somites and tail bud, albeit with a very low efficiency (<1%) and the organ primordia exhibiting notable defects[70–72].

Assembloids have also emerged as scalable and controllable models to generate peri-gastrulation mouse embryo models[28,74] (Table 1). Assembloids are 3D structures formed by fusing two or multiple spheroids to model tissue–tissue interactions[75,76]. However, due to their simple tissue organization, assembloids might be limited in modelling the complex cytoarchitecture formed through dynamic pattern formation processes in natural embryos. For example, to model peri-gastrulation mouse development, mouse ES spheroids TSC spheroids were assembled to guide their interaction, leading to the formation of regionalized mesodermal cells in mouse ES cell spheroids with an efficiency of 50–70%[74]. Similarly, assembling a mouse ES cell cluster and another one pre-treated with BMP4 (as a signalling centre secreting WNT and NODAL signals) efficiently (>90%) generated peri-gastrulation mouse embryo models with well-delineated orthogonal A–P and D–V body axes and patterned germ layer lineages[28]. This model further formed organ primordia comparable to those in neurula-stage mouse embryos, including the neural tube, gut tube, somitic and intermediate mesodermal tissues, cardiac tissues, and a vasculature network[28].

Peri-gastrulation human embryo models were first developed from primed hPS cells without involving extra-embryonic cells[77–79] (Table 1). For example, a subset of primed hPS cell clusters in 3D Matrigel spontaneously underwent epithelization and lumenogenesis, giving rise to a lumenal epithelial structure, prior to 5–10% of structures spontaneously breaking symmetry to form a bipolar structure mimicking early post-implantation EPI and amniotic ectoderm patterning[79]. This model was termed post-implantation amniotic sac embryoid (PASE)[79]. Some of the PASE structures progressively developed, with the EPI-like compartment undergoing EMT and giving rise to mesodermal lineages[79]. Using microfluidic devices to provide asymmetric external morphogen stimulations to primed hPS cell clusters substantially improved the efficiency of PASE formation (~90%)[29]. Confirmed in peri-gastrulation primate monkey embryos[80], paracrine signalling (likely BMP signals downstream of *ISL1*) from amniotic cells is involved in driving the gastrulation process in the EPI[29,80],

Recently, numerous peri-gastrulation human embryo models have incorporated both embryonic and extra-embryonic compartments such as a yolk sac-like structure and trophectoderm derivatives[81–87] (Table 1 and Fig. 1d). Some of these models suggest that yolk sac endoderm-like cells might secret BMP and WNT antagonists to promote anterior ectoderm formation[81–87], supporting the notion that, in humans, there are yolk sac endoderm cells functioning similarly to the mouse AVE to induce symmetry breaking and A–P patterning of peri-gastrulation human EPI. Nonetheless, these models still suffer from low efficiencies in modelling these events and forming in vivo-like tissue structures.

Morphogen-mediated neural tube patterning and its modelling. During gastrulation, embryonic germ layer subpopulations in the mammalian embryo come together, facilitating interactions that shape tissue layers, specify cell types and initiate organ rudiment development. A critical event in the embryonic ectoderm after gastrulation is neural tube formation and patterning, laying the foundation of the functional complexity and anatomical organization of the human nervous system. Patterning of the neural tube along the A–P axis leads to the formation of four main subdivisions: forebrain, midbrain, hindbrain and spinal cord (Fig. 1e). D–V patterning of each neural tube subdivision gives rise to various neuronal progenitor cells along the D–V axis. For example, D–V patterning of the spinal cord results in the formation of 11 neural progenitor domains — 5 ventral and 6 dorsal — each expressing a specific combination of transcription factors that constrain their lineage development.

Knowledge of neural tube patterning mostly comes from chick and mouse embryo studies. The axial patterning of the neural tube involves external morphogen gradients, which establish positional information across the tube along both the A–P and D–V axes. A–P patterning is mainly governed by P–A gradients of posteriorizing signals, including WNT, retinoic acid and FGF[88–90] (Fig. 1e). A–P patterning of the neural tube is further refined by developmental signals emanated from secondary organizers such as FGF signals from the anterior neural ridge and the isthmic organizer at the midbrain–hindbrain boundary[91] (Fig. 1e). D–V patterning of the neural tube is mainly mediated by antiparallel gradients of BMP, WNT and sonic hedgehog (SHH) along the D–V axis[92,93] (Fig. 1e). BMP and WNT molecules are secreted by dorsal non-neural

ectoderm and subsequently by the roof plate, whereas SHH is emanated from the ventral notochord and subsequently by the floor plate[92,93] (Fig. 1e). Retinoic acid secreted from the paraxial mesoderm and somites flanking the neural tube is also important for ventral patterning[94].

Stem cell-based neural tube patterning models have been developed with both mouse ES cells and hPS cells, leveraging their self-organizing pattern formation properties[95–97] (Table 1). Seeded in Matrigel or synthetic poly(ethylene glycol) (PEG)-based hydrogels under neural induction culture conditions, both mouse ES cells and hPS cells formed spherical lumenal neuroepithelial cysts containing a single central lumen[95–97]. Supplementing the ventralizing signals retinoic acid and/or SHH into culture medium induced D–V patterning of neuroepithelial cysts, featuring sequential emergence of the ventral floor plate, P3 and pMN domains in discrete, adjacent regions and a dorsal territory progressively restricted to the opposite dorsal pole[95,96]. It remains unclear how applying exogenous ventralizing morphogens leads to self-organized, D–V patterning of neuroepithelial cysts. At the initial phase of D–V patterning, FOXA2$^+$ floor plate progenitor cells emerge first in neuroepithelial cysts but in a scattered fashion[95,96]. Soon thereafter, FOXA2 expression becomes restricted to a local floor plate-like region, defining the ventral pole of neuroepithelial cysts[95,96]. This FOXA2$^+$ floor plate-like domain might function as a local signalling centre to induce and pattern other ventral regions in both mouse and human neuroepithelial cysts[95,96]. Moreover, self-organized D–V patterning of mouse neuroepithelial cysts might involve interactions of BMP and Noggin with a reaction–diffusion-based Turing patterning mechanism[98,99]. Whether such self-organizing mechanisms operate in vivo for axial patterning of the neural tube is unclear. PEG-based hydrogel systems with tuneable degradability, stiffness and matrix composition were used in D–V patterning of mouse neuroepithelial cysts to disentangle the contributions of individual biochemical and physical components of the microenvironment[97]. Nevertheless, D–V patterning of mouse and human neuroepithelial cysts under uniform culture conditions remains inefficient (30–40%).

Microfluidics technologies provide precise spatiotemporal control of chemical signals and can be used to create morphogen environments for different neural tissue engineering applications, including improving patterning efficiency of stem cell-based neural tube development models[30,31] (Table 1). For example, D–V patterned human forebrain organoids derived from hPS cells were generated by culturing embryonic bodies under a SHH gradient generated in a passive diffusion-based microfluidic gradient generator[100]. Another microfluidic device that employed a series of splitting and mixing of microfluidic flows was used to generate a linear WNT signal gradient across 2D layers of hPS cells[30], resulting in an A–P patterned human neural tube development model with progressive caudalization from forebrain to midbrain to hindbrain[30]. Notably, an isthmic organizer-like domain spontaneously emerged between the midbrain-like and hindbrain-like regions, further highlighting the autonomous and self-organizing properties of neural tube development, leading to the formation of local secondary organizers at subdivision boundaries[30].

A–P and D–V patterned neural tube-like structures have been recently generated, termed microfluidic neural tube-like structure or μNTLS[31]. Specifically, tubular-shaped hPS cell tissues were grown in a microfluidic chamber, in which morphogen gradients were established through passive diffusion of different morphogens added to medium reservoirs connected to the chamber[31]. Orthogonal morphogen gradients were established: one consisting of WNT, retinoic acid and FGF8 signals along the length of μNTLS to induce its A–P patterning and the other of antiparallel BMP4, retinoic acid, and SHH signals perpendicular to the μNTLS length to induce its D–V patterning (Fig. 1f). Importantly, the μNTLS was used to study neuronal lineage development, revealing pre-patterning of axial identities of neural crest progenitors and functional roles of neuromesodermal progenitors (NMPs) in spinal cord and trunk neural crest development. Thus, stem cell-based neural tube development models using microfluidics with in vivo-like spatiotemporal cell differentiation and organization are promising tools for the study of human neurodevelopment and disease.

Bioengineering tools to guide pattern formation

Bioengineering approaches can be used to control cell number and geometries of morphogenetic fields, tissue–tissue interactions (including both paracrine and juxtacrine interactions), and external chemical gradients. Thus, they could improve the efficiency and fidelity of both self-organized and external cue-guided tissue patterning modelling in stem cell-based embryo models.

Controlling initial cell cluster formation. Commercial AggreWell and micropatterned agarose microwell plates have been used for blastoid and other embryo model developments, including ETS and ETX models[24,53–57,67–69] (Fig. 2a). These confining microwell plates improve efficiency and throughput by promoting cell aggregation and cell–cell interactions. However, AggreWell only allows control over the size but not the geometry of initial cell aggregates, an issue that can be addressed by using 3D hydrogel microwells fabricated by moulding or laser ablation of hydrogels such as collagen or Matrigel[101,102]. The pyramidal shape of AggreWell also limits high-resolution in situ imaging of free-floating embryo models, which requires two-photon light sheet microscopy. By contrast, microfluidics can control initial cell cluster formation and are compatible with high-resolution imaging; for example, they enabled accurate control of size and location of hPS cell clusters with defined cell numbers by aggregating hPS cells in preformed concave hydrogel pockets for PASE development[29]. Moreover, live imaging was conveniently conducted to track tissue morphogenetic events, including symmetry breaking and signalling dynamics using reporter cell lines[29].

During development, pattern formation is often followed by tissue growth and functional maturation of organs. Despite their versatility, microfluidic devices are not suitable for long-term culture and continuous growth of embryo models. Integrating microfluidics with conventional tissue cultures to promote long-term growth of spatially patterned embryo models can be foreseen, with initial cell cluster formation and tissue patterning conducted in microfluidic devices, followed by transfer of embryo models to conventional culture systems for continuous development and tissue growth.

Bioengineered co-culture systems to guide tissue–tissue interactions. A co-culture system should satisfy three key criteria: (1) enable accurate control of the proportions of each cell type within specific regions of the co-culture, (2) enable efficient cell–cell interactions (paracrine or juxtacrine interactions) and (3) facilitate co-development of different cell types.

Micropatterning-based co-culture platforms, which rely on polydimethylsiloxane stencils or microcontact printing, have been developed to precisely control spatiotemporal organizations of two or more different adherent cell types in 2D cultures[103–106]. Unlike stencil

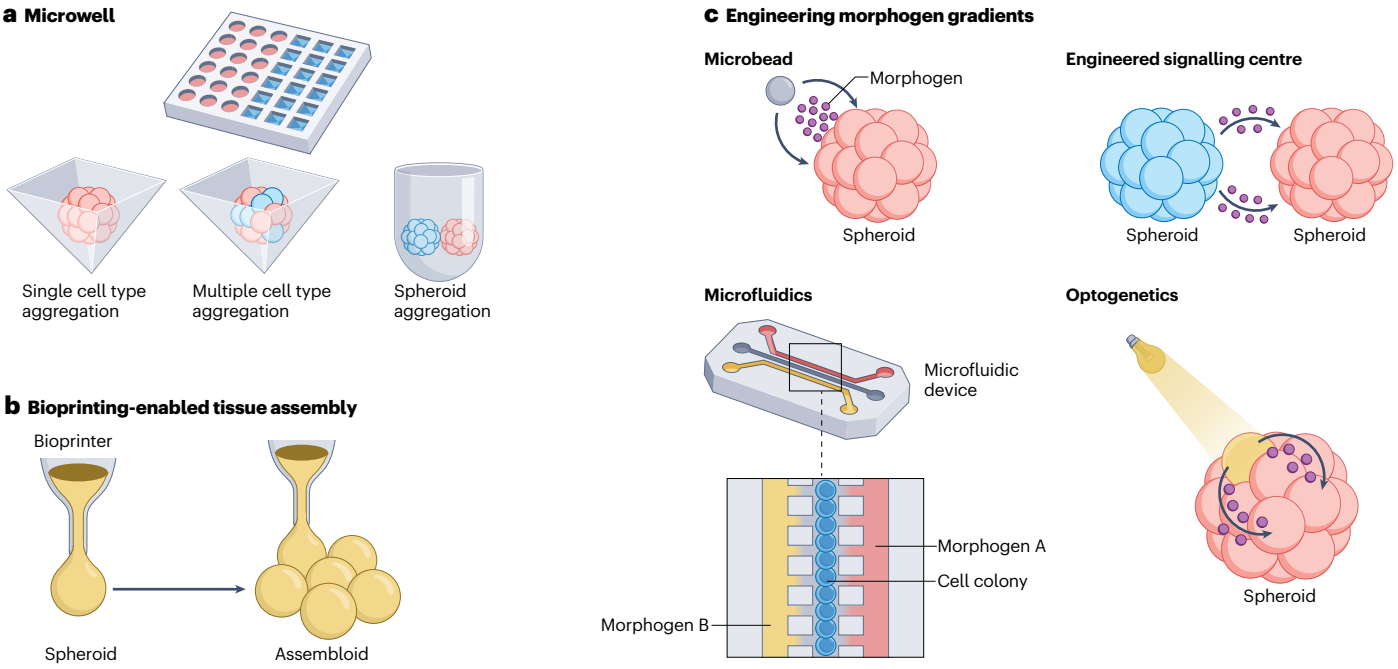


Fig. 2 | Bioengineering approaches for guiding pattern formation in embryo models. a, Microwells to promote cell and spheroid aggregation. **b**, 3D bioprinting to assemble spheroids into complex structures. **c**, Engineering signalling centres and morphogen gradients through porous microbeads, optogenetics, engineered signalling centres and microfluidics.

micropatterning[104–106], microcontact printing-based co-cultures can physically separate and control the spacing between different cell types[103], making them suitable for decoupling juxtacrine and paracrine interactions. Micromachined silicon substrates with controllable moving parts also enable dynamic control of tissue organization and composition through mechanical repositioning, and have been used to investigate dynamic cell–cell interactions in co-cultures of hepatocytes and non-parenchymal cells[107]. Micropatterning-based co-culture platforms are also compatible with many other microengineering and mechanobiology tools such as microfluidic gradient devices[108], tissue stretching devices[109], microfabricated pillar force sensor arrays[109] and surface biosensing techniques[110]. Integrating these tools will enable control, perturbation and quantification of physicochemical cues involved in tissue–tissue interactions during embryo modelling. For example, amnion functions as a signalling centre secreting BMP and/or WNT molecules to drive gastrulation in primates[29,80]. However, the molecular mechanisms underlying the amnion–EPI interaction are unclear, and it is challenging to use primate embryonic tissues for this purpose. In the future, an amnion–EPI co-culture model could be developed using micropatterning to study the role and nature of such interactions in driving primate gastrulation. Moreover, integrating this platform with surface biosensors could provide information about paracrine or juxtacrine interactions between the two tissues during primate gastrulation. Direct measurements of BMP and WNT ligands, in combination with genetic and chemical perturbations, in the amnion–EPI co-culture model could shed light on the molecular mechanisms underlying inductive effects of amnion on human EPI development.

However, 2D co-cultures are limited to studying intercellular and tissue–tissue communications in 2D settings. Transitioning from 2D to 3D cell cultures, 3D bioprinting enables precise and flexible assembly of living cells, tissues, biomaterials and other bioactive molecules into complex 3D structures, replicating the intricate architecture of biological tissues or organs[111] (Fig. 2b). Despite not being applied for embryo modelling, 3D bioprinting has been used to develop other high-cell density heterogeneous tissue models[112]. For example, magnetic-assisted or aspiration-assisted bioprinting are embedded 3D bioprinting methods that use magnetic forces or aspiration to transfer tissue spheroids into self-healing support hydrogels at high resolution, enabling patterning and fusion into high-cell density microtissues of prescribed spatial organization[113,114] (Fig. 2b). This method was applied to develop co-cultures of hPS cell-derived cardiomyocytes and cardiac fibroblasts to recapitulate structural and functional features of cardiac tissues[113]. Similarly, perfusable vascular channels were printed into large organ-specific spheroids using embedded 3D bioprinting to promote their long-term growth and maturation[115].

Controllable and reproducible tissue co-culture platforms with prescribed spatial tissue organizations, based on either 2D micropatterning-based systems or 3D bioprinting, therefore have great potential for building advanced embryo models.

Engineering signalling centres and morphogen gradients. Chemical signals, often in the form of signalling molecules such as growth factors and morphogens, guide cellular behaviours, ensuring proper organization and specialization of cells for the formation of functional tissues and organs during development. Manipulating the distribution and timing of chemical signals in vitro is crucial for advanced embryo modelling. Some of these methods include chemical-soaked microbeads[116,117], microfluidics[27,118,119], engineered

morphogen-secreting signalling centres[28,120,121] and optogenetics[122,123] (Fig. 2c).

Microbeads, when loaded with growth factors, hormones, or morphogens and placed near developing tissues or embryos, are often used to create controlled microenvironments and study the effects of localized chemical signals and their gradients on developing tissues or organisms (Fig. 2c). For example, chemical-soaked microbeads were used to study morphogen-guided pattern formation in amphibian embryos[124,125]. Similarly, CHIR99021 (a WNT agonist)-soaked and BMP-soaked agarose beads were placed adjacent to human brain organoids to induce localized dorsal cortical hem-like identities in the organoids[116].

Localized signalling centres can also be generated by engineering cells either chemically or genetically. Treating mouse ES cells with BMP4 upregulates *Nodal* and *Wnt3* expression; therefore, clusters of BMP4-treated mouse ES cells could serve as a signalling centre emanating NODAL and WNT signals. Assembly of BMP4-treated mouse ES cell clusters with wild-type mouse ES cell clusters generated a mouse embryo model that recapitulated the formation and organization of the three embryonic germ layer derivatives[28] (Fig. 2c). In another study, genetically modified, chemically inducible SHH-secreting hPS cells were placed on one side of human brain organoids; in the presence of doxycycline, the cells secreted SHH to guide the patterning of human brain organoids to form spatially restricted forebrain subregions, including regions resembling the ganglionic eminence, hypothalamus, thalamus and dorsal forebrain[120].

Despite their simplicity, it is difficult to control the range, slope and temporal dynamics of morphogen gradients using chemical-soaked beads and engineered signalling centres, thus limiting quantitative studies of morphogen signals and their roles in pattern formation and other developmental processes. These limitations can be addressed by using microfluidics, which can control spatiotemporal distribution of signalling molecules and thus create signalling gradients with precise ranges and slopes (Fig. 2c). For example, microfluidics has been used to induce WNT signal gradients to generate an A–P patterned human neural tube model[30], a linear SHH gradient to generate D–V patterned human forebrain organoids[100], or orthogonal morphogen gradients to a A–P and D–V patterned neural tube model[31]. However, microfluidic device design and fabrication are complex and require specialized knowledge in microfabrication techniques. Developing user-friendly platforms, promoting standardization and cross-collaboration between engineers and biologists might help boost the adoption of microfluidics in embryo modelling and organoid research[27,126].

Optogenetics is another useful approach for establishing exogeneous morphogen gradients, for example, by inducing a subpopulation of cells to produce specific morphogen signals through photoactivation of transcription factors with high spatiotemporal precision (potentially greater than microfluidics)[127] (Fig. 2c). For instance, local optogenetic activation of SHH in a human spinal cord organoid robustly induced spatially organized ventral spinal cord domains surrounding SHH-secreting cells[122,128]. Nonetheless, certain limitations, including off-target effects, limited tissue penetration and phototoxicity, still need to be addressed for reliable optogenetics-mediated transcriptional control[129].

Tissue morphogenesis

Morphogenesis is required for tissues and organs to acquire 3D structures during development. This process is achieved by coordinated cellular activities such as cell division, adhesion, migration and changes in cell shape. Cell–cell adhesive interactions maintain tissue boundaries and enable tissue-level cell arrangements and movements. Loss of cell–cell adherens junctions between epithelial cells leads to EMT as in the primitive streak formation during gastrulation[130]. Conversely, formation of adherens junctions between mesenchymal cells results in mesenchymal-to-epithelial transition (MET), as in the condensation and segmentation of presomitic mesoderm (PSM) to form somites[131]. In vitro, cell–cell adhesions can be engineered using synthetic biology approaches to facilitate tissue assembly to build multicellular structures (see Synthetic biology for embryo models for more discussions). Cell shape change and migration, which are regulated by intracellular cytoskeleton dynamics, are crucial in many morphogenetic events such as gastrulation and neurulation[130,132]. Cell shape can be modulated by geometrical confinement (such as micropatterning) and mechanical perturbations (such as tissue stretching), as demonstrated in 2D micropatterned gastrulation and neural development models[25,109].

Cell–ECM interactions also have an important role in tissue morphogenesis by influencing cell shape, polarity and organization as well as migration during processes such as gastrulation and organogenesis[133,134]. Besides providing mechanical support and promoting tissue integrity, cell–ECM interactions also modulate various signalling pathways, influencing processes such as proliferation, survival and differentiation[133,134]. When embedded in natural or synthetic hydrogels, morphogenetic events were triggered in different embryo models mimicking neurulation and somitogenesis, highlighting the role of cell–ECM interactions[135–137].

Morphogenesis in vivo and in embryo models

Gastrulation: forming an organized body plan. As a highly orchestrated process, gastrulation lays the foundation of the basic body plan[33,64,130]. Besides germ layer lineage fate specification, gastrulation involves a myriad of morphogenetic events to organize the topology of the three definitive germ layers; these morphogenetic events include EMT, cell migration, convergent extension and elongation along the A–P axis[130,138] (Fig. 3a). Much attention has been paid to mimicking germ layer lineage differentiation and patterning in peri-gastrulation embryo models established using 2D micropatterned hPS cell colonies treated with exogeneous BMP4 (ref. 25) (Table 1 and Fig. 3b). These 2D human gastrulation models are compatible with live imaging and can be generated robustly. Therefore, they enable quantitative studies to elucidate the mechanisms underlying germ layer lineage patterning, including dynamic waves of BMP, WNT and NODAL signalling, interaction of endogenous activators and inhibitors in a diffusion-reaction mechanism, and basolateral localization of BMP receptors[23,139,140]. The latter was further shown to have a role in the formation of a robust BMP signalling gradient in peri-gastrulation mouse embryos[141].

3D gastrulation models, or gastruloids, have been generated by treating 3D clusters of mouse ES cells or hPS cells with a pulse of WNT agonist CHIR99021, forming an A–P axis and differentiated germ layer derivatives spatially organized along this axis[135,142–144] (Table 1). More advanced gastruloids recapitulate the formation of organ primordia during early organogenesis, such as the neural tube, bilateral somites, gut tube and cardiac tissues, by optimizing chemical and mechanical signals in culture[137,145,146] (Table 1). Tissue organization and patterning in gastruloids were achieved without the presence of extra-embryonic lineages, suggesting self-organized pattern formation mechanisms at play. Other post-implantation and peri-gastrulation human embryo

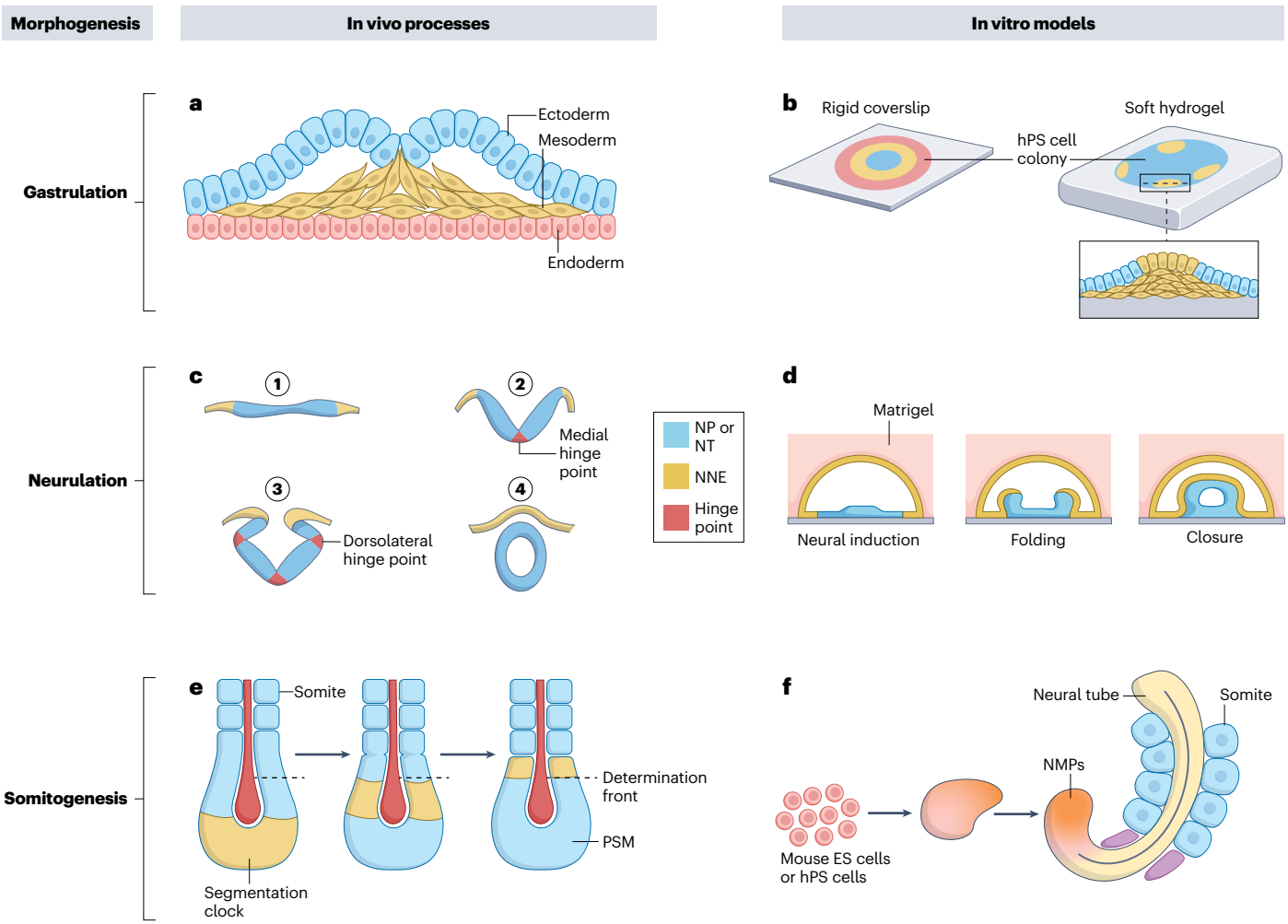


Fig. 3 | Morphogenesis in vivo and in embryo models. In vivo process and in vitro modelling of gastrulation, neurulation and somitogenesis. **a**, Gastrulation involves different morphogenetic events, such as epithelial–mesenchymal transition, cell migration and axial elongation, to organize the topology of three embryonic germ layers. **b**, 2D micropatterned human pluripotent stem (hPS) cell colonies treated with BMP4 develop into concentric rings of three germ layers, recapitulating cell fate patterning during gastrulation[25]. Culturing micropatterned 2D gastrulation models on a soft hydrogel promotes gastrulation-like morphogenesis, such as ingression and migration of mesoderm cells[148]. **c**, Bending and closure of the neural plate (NP) during neurulation. NP bending is mainly driven by mechanical forces generated by apical constriction in NP cells at the median and dorsolateral hinge points. **d**, A neurulation model established by combining micropatterned 2D hPS cell colonies with 3D culture to recapitulate NP folding and closure[136]. **e**, Somite formation during somitogenesis, which can be explained by the clock-and-wavefront model. In this model, somitogenesis is regulated by the combined action of a molecular segmentation clock and a moving determination front of FGF and WNT signalling activities. **f**, Co-morphogenesis of neural tube (NT) and somite-like structures in mouse or human embryo models[137,177]. ES cell, embryonic stem cell; NMP, neuromesodermal progenitor; NNE, non-neural ectoderm; PSM, presomitic mesoderm.

models have also incorporated putative extra-embryonic signalling centres such as the amnion-like, yolk sac-like and trophectoderm-like derivatives[81–87] (Table 1). These models are promising in studying how self-organized patterning mechanisms function synergistically with embryonic–extra-embryonic interactions to ensure the robustness of the gastrulation process and embryonic germ layer organization.

Emerging evidence suggests that cell fate patterning and morphogenesis might be regulated independently during gastrulation[130,147]. This observation is corroborated by findings from 2D and 3D gastrulation models, which recapitulate spatially patterned germ layer fate organization without notable morphogenetic events. Nonetheless, how cell fate patterning and morphogenesis are coordinated to establish the body plan during gastrulation remains ill-understood. Stem cell-based embryo models that can mimic both cell fate patterning and morphogenetic events during gastrulation are thus promising for elucidating this important question. To promote morphogenetic events, bioengineering approaches have been integrated with gastrulation models. For example, culturing micropatterned 2D human gastrulation models on a soft polyacrylamide hydrogel that recapitulated the biophysical properties of early embryos promoted 'gastrulation-like' morphogenesis of hPS cells, including self-organization of 'gastrulation-like' nodes and ingression and migration of mesoderm cells through these nodes[148] (Table 1 and Fig. 3b). Moreover, tissue geometries dictated the formation of nodes in regions of high cell-adhesion tension, which promoted

WNT signalling and mesoderm specification. Furthermore, mechanical stretching could promote mesoderm specification, confirming the role of tissue-level forces in regulating lineage differentiation during gastrulation[149,150].

Without extra-embryonic tissues, there is no primitive streak-like structure formation in gastruloids[138,144]. Other morphogenetic events, such as collective cell migration, also do not seem to occur in gastruloids[138,144]; however, when co-culturing mouse ES cells with extra-embryonic cells, such as mouse TSCs and/or XENs in ETS and ETX embryo models, a primitive streak-like structure emerged in the compartment of mouse ES cells adjacent to mouse TSCs[68] (Table 1). Similarly, in a 3D human peri-gastrulation model including both embryonic and extra-embryonic tissues, a putative primitive streak-like structure emerged at the posterior end of the model, characterized by cells undergoing EMT and inward migration[83] (Table 1). These studies suggest that the primitive streak might be a transient structure whose formation depends on the mechanics and geometrical boundary constraints imposed by adjacent extra-embryonic tissues[130,138]. Using bioengineering approaches to control tissue mechanics and topology in embryo models will be an important direction to study the morphogenetic events that occur during gastrulation.

A well-recapitulated morphogenetic event in gastruloids is axial elongation. Along the A–P axis, peri-gastrulation embryo elongates, with progenitors in the tail bud proliferating and differentiating to give rise to tissues that generate posterior spinal cord, skeleton and musculature[151]. In gastruloids, axial progenitors (likely including NMPs) emerge at their posterior ends, give raise to both neural and mesodermal lineages, and contribute to posterior elongation of gastruloids[135,137,142–144]. In mouse gastruloids, P–A gradients of Erk and Akt signals control unidirectional tissue growth at their posterior ends by modulating cell proliferation, motility and adhesion[152]. Tissue elongation and narrowing along the A–P axis, which resembles convergent extension during mouse gastrulation, was also observed in mouse gastruloids and confirmed in silico[153]. In vivo, convergent extension is a complex process involving molecular and cellular events that coordinate cell movements and rearrangements, including cell polarization, dynamic changes of cell adhesion and cytoskeleton, cell intercalation, and planar cell polarity signalling[154]. It will be important to examine whether these molecular and cellular events are involved in the axial elongation of gastruloids.

Neurulation: tissue bending morphogenesis. Neurulation describes the developmental process through which the neural tube is formed from the neural plate specified in the ectoderm. After gastrulation, the ectoderm is specified into the neuroectoderm, containing the neural plate, flanked by the neural plate border and non-neural ectoderm (NNE), through the process of neural induction. As neurulation progresses, the neural plate undergoes structural changes, with the lateral edges of the plate elevating to form two parallel ridges called neural folds (Fig. 3c). The neural folds eventually meet in the dorsal midline of the embryo and fuse to form the hollow neural tube, which contains a central lumen called neural canal (Fig. 3c). In mammals, neural plate bending is primarily driven by mechanical forces generated by apical constriction in the cells at the median and dorsolateral hinge points[132] (Fig. 3c). Proliferation of NNE tissues also generates mechanical forces to facilitate neural plate bending and closure[132]. Once the two opposing neural folds meet at the dorsal midline, cells at the tips of the neural folds develop cellular protrusions to attach to the opposite neural folds. The neural tube then becomes separated from the dorsal NNE tissue due to differential adhesions. The dynamics of neurulation depends on the A–P axial level[132]; fusion of neural folds begins in the middle of the embryo and moves anteriorly and posteriorly[132]. Disruption of several actin-associated proteins prevents bending of the neural plate only in anterior regions but not in spinal regions[155–158], supporting different dynamics and regulatory mechanisms of neurulation at different A–P axial levels.

Neurulation is a tightly regulated process, disruption of which can lead to neural tube closure defects (NTDs), one of the most common congenital disorders affecting the nervous system. Genetic mutations affecting BMP, SHH, WNT and planar cell polarity signalling pathways, impaired cell proliferation, apoptosis and ECM formation, abnormal cell adhesion, migration and actomyosin turnover, oxidative stress and inflammation, and environmental factors have all been implicated in NTDs[158–161]. Understanding the molecular and cellular mechanisms underlying neurulation is essential to inform the aetiology of NTDs.

Neurulation studies have mainly been conducted using chick and mouse embryos but hPS cell-based neurulation models are emerging[109,136,162–165] (Table 1). Neural rosettes are 2D neuroepithelial tissues derived from hPS cells whose initial tissue geometry is crucial for proper lumen formation. The lumenal morphology of human neural tubes was therefore modelled using micropatterned 2D neural rosettes containing a single central lumen[162,166] (Table 1). A similar approach recapitulated neuroectoderm patterning and even the single lumen morphology of the neural tube[109,163,164] (Table 1). Notably, self-organized morphogenetic cues, including cell shape and cytoskeletal contractility, could directly feedback to mediate BMP activity to guide spatial neuroectoderm patterning[109]. Thus, these models reveal an intricate signalling crosstalk involving both biophysical and biochemical factors that might control neuroectoderm patterning networks in vivo.

However, 2D micropatterned neurulation models are not fully representative of 3D neural plate folding morphogenesis. Combining micropatterned 2D hPS cell colonies with a 3D culture in Matrigel recapitulated neuroectoderm patterning followed by the dynamic neural plate folding and fusion process at a 90% success rate, efficiently forming a 3D tubular structure mimicking the cranial neural tube[136] (Table 1 and Fig. 3d). This model further demonstrated the impact of chemicals perturbing apical constriction and basal ECM synthesis on folding and closure of the neural plate.

Spinal cord organoids derived from hPS cells also recapitulate neurulation-like tube-forming morphogenesis of the early spinal cord[165] (Table 1). Specifically, caudalized 2D hPS cell colonies, likely through a transient NMP stage, were detached from 2D cultures to form 3D spheroids induced with a neuroepithelial fate in a free-floating culture. Neural plate-like structures spontaneously emerged on the surfaces of these spheroids and underwent folding morphogenesis to form such structures within the 3D spheroids, likely involving apical constriction in neuroepithelial cells[165]. This process occurred in the absence of neural plate border or NNE tissues, supporting the role of innate self-organizing properties of neural plate cells in driving their folding dynamics[165].

Somitogenesis: tissue segmentation morphogenesis. Somitogenesis is the process by which somites are formed in the embryo. Somitogenesis establishes the segmented pattern of the vertebrate body plan, essential for proper formation and function of the musculoskeletal system. Defects or disruptions in somitogenesis could lead to congenital abnormalities such as scoliosis. Somitogenesis has mainly

been studied in chick and mouse models; during this process, the PSM, a bilateral strip of mesenchymal tissue flanking the forming neural tube, progressively segments into bilaterally symmetrical epithelial somites in the A–P direction[131] (Fig. 3e). Somitogenesis can be explained by the clock-and-wavefront model, which proposes that somitogenesis is regulated by the combined action of a molecular clock mechanism within the PSM and a moving wavefront of signalling activity along the A–P axis[131] (Fig. 3e). This model provides a conceptual framework for understanding how the periodic segmentation of somites is controlled during embryonic development.

Somitogenesis is an excellent developmental process to study the formation of morphological boundaries between developing tissues; new somites are formed at the anterior end of the PSM, where cells undergo MET and coalesce into a rosette-like structure that pulls apart from the PSM. Specifically, anterior PSM cells undergo changes in cell adhesion, cell shape and cell–cell interactions, contributing to the morphological formation of an intersomitic boundary (also called a fissure) and separation of forming somites from the PSM[167]. Fissure formation in somitogenesis is an intrinsic property of PSM cells and does not rely on surrounding tissues[168]. After its formation, PSM cells in the somite undergo MET, resulting in the conversion of loosely packed mesenchymal cells into tightly packed epithelial ones, which contribute to the structural integrity of somite boundaries[167]. Besides classic morphogenetic studies of somitogenesis, studies using chick embryos have revealed decreasing cell stiffness, polarity and adhesion along the A–P axis in the chick PSM[169]. Moreover, applying external mechanical stress along the A–P axis of the chick PSM induced the formation of new somite boundaries that were not determined by the clock-and-wavefront model, suggesting that mechanical cues could also be instructive for somite formation[170,171].

Somitogenesis was first recapitulated in gastruloids; when embedded in Matrigel, mouse gastruloids (termed trunk-like structures) developed a neural tube-like structure flanked by the PSM and epithelial somite-like tissues[137] (Table 1 and Fig. 3f). Similar human somitogenesis models were developed by culturing hPS cell clusters in PSM differentiation environments[172–175] (Table 1). These models exhibit oscillatory expression of clock genes in the PSM, periodic epithelialization and segmentation of somites, and A–P polarity in each single somite. Moreover, they revealed an unexpected role of cell sorting in somite formation and of retinoic acid in the epithelialization of somites[174,175]. Notably, Matrigel appeared to be critical for the epithelialization of somitic cells but was not required for somitic differentiation of PSM cells in either mouse or human somitogenesis models[137,174,175].

To study the biochemical–biomechanical interactions that drive somitogenesis, another somitogenesis model was developed in a microfluidic device by controlling exogenous antiparallel retinoic acid and WNT–FGF signalling gradients and mechanical boundaries in hPS cell-derived PSM tissues[176] (Table 1). A fracture mechanics-based theoretical model, which considered strain energy induced by compaction of a forming somite and surface energy resulting from a new somite–PSM boundary, was proposed to explain the size dependency between somites and the PSM, which is observed in mouse, chick, zebrafish and human embryos.

Co-morphogenesis of neural tube-like and somite-like structures was also achieved in mouse and human trunk-like structures under a transient WNT signal stimulation and Matrigel embedding[137,177] (Table 1 and Fig. 3f). In vivo, posterior spinal cord and somites originate from a common caudal progenitor population, including NMPs. Mouse and human trunk-like structures, which recapitulate the spatiotemporal development of these three lineages, could be useful to study their lineage relationships and the genetic and molecular mechanisms underlying caudal lineage diversifications.

Bioengineering tools to guide morphogenesis

In vivo and in vitro studies have highlighted the role of geometrical tissue boundary conditions in providing a ground state for morphogenetic events[130,138]. Thus, strategies that can control the geometrical boundaries of 2D and 3D tissues can be used to engineer tissue morphogenesis and improve the efficiency and robustness of embryo and organ model developments. Synthetic biomaterials engineered with specific mechanical properties and/or functionalized with growth factors and adhesive signalling molecules can further guide this process.

Engineering tissue geometry and boundary. Micropatterning (including microcontact printing[178], stencil micropatterning[179,180] and photopatterning[25]) can generate 2D cell colonies with controlled size, shape and physical boundary conditions by creating patterns of adhesive molecules to enable selective cell attachment (Fig. 4a). Microcontact printing is the process of printing adhesive islands onto substrates using stamps[178]. Adhesion properties, surface energy and chemical compatibility between the stamp, printed adhesive molecules and substrates must be carefully considered to ensure successful pattern transfer.

Stencil micropatterning instead involves the use of stencils, which are essentially masks with specific patterns or designs cut out of them. These stencils are placed onto a substrate, and material is deposited

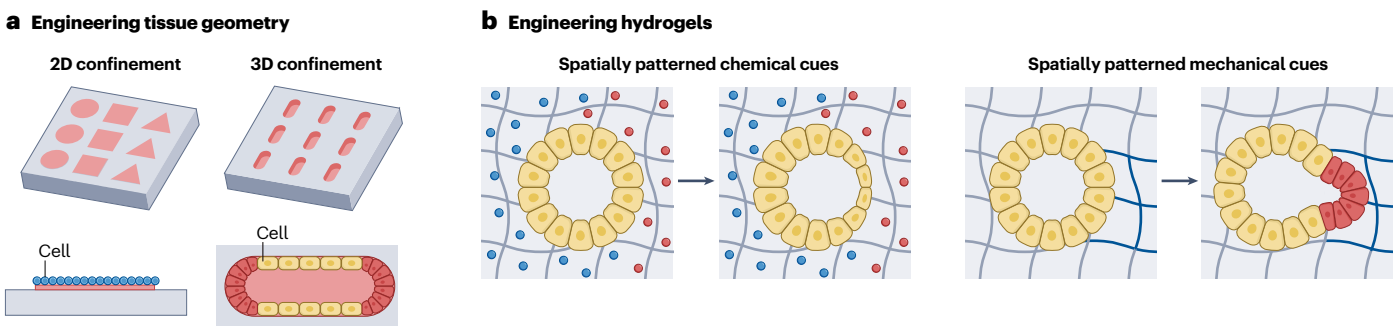


Fig. 4 | Bioengineering approaches to guide morphogenesis in embryo models. a, Engineering tissue geometry and boundary using micropatterning tools. **b**, Synthetic hydrogels with engineered spatially patterned chemical and mechanical cues.

or removed through the openings in the stencil to create desired patterns on the underlying surface. Thus, in stencil micropatterning, the stencil-to-substrate contact is important in determining pattern fidelity and reproducibility. Stencil micropatterning can be used to generate micropatterned 2D cell colonies by applying stencils onto cell culture substrates before cell seeding[179,180]. After cell seeding, stencils can be removed to release the geometrical constraints on the growing cell colonies. This technique is best suited for simple geometric patterns with well-defined shapes and features. However, similar to microcontact printing, stencil micropatterning typically provides static, fixed patterns on substrates. Moreover, the static control over pattern geometry limits the applicability of stencil micropatterning and microcontact printing for studying the effect of dynamic geometrical changes in tissue morphogenesis such as in crypt formation during intestinal development.

In photopatterning, cell culture surfaces coated with a layer of cytophobic or cell-repellent molecules are patterned using UV light passing through a photomask[181–183]. Localized UV light exposure of cytophobic molecules promotes their degradation and exposes underlying cell culture surfaces for subsequent functionalization with adhesive molecules to promote local cell attachment[181–183]. Similar to previous techniques, photopatterning typically involves patterning cells at a single time point, resulting in static, fixed patterns. It also relies on photosensitive materials whose long-term cytotoxic effects and degradation properties need to be evaluated. Micropatterned cell culture surfaces generated using photopatterning are commercially available, which promotes their broader applications especially in labs that lack access to microfabrication facilities[25].

Integrating 2D micropatterning tools and 3D culture can expand their application to model 3D morphogenetic events such as tissue folding and fusion[136]. Moreover, 3D structures made of polydimethylsiloxane or hydrogels containing channels or wells of defined sizes and shapes (fabricated by soft lithography or laser ablation) have also been used to guide morphogenetic events involved in somitogenesis and intestinal morphogenesis[101,102,176] (Fig. 4a). Given their superior reproducibility, scalability and compatibility with live imaging, micropatterned 2D or 3D culture systems are promising for translational applications such as drug and toxicity screens.

Bioengineering hydrogels. In vivo, the ECM provides structural support, mechanical stability and biochemical signalling cues to guide morphogenetic events during embryonic development. Matrigel, a gelatinous protein mixture extracted from Engelbreth–Holm–Swarm mouse sarcoma, is the most widely used natural ECM for 3D cultures, including embryo and organ model cultures. However, Matrigel is an ill-defined material with substantial batch-to-batch variations, which limits reproducibility[184]. Moreover, Matrigel offers no direct control over its molecular composition or components, making it unsuitable for studying the role of individual ECM components in regulating embryonic development[184]. Because Matrigel is derived from animals, there is a risk of contamination with animal-derived factors, which further limits its clinical application[184].

Alternatively, synthetic biomaterials incorporating bioactive molecules, cell-adhesive motifs and tissue-specific cues can mimic the structure and function of natural ECMs more adaptably. Synthetic matrices, such as PEG-based hydrogels, have already been used in mouse and human intestinal organoids and D–V patterned mouse neural tube development models[97,185–187]. Besides modulating biochemical properties, they enable independent modulation of biophysical properties such as degradability, porosity and viscoelasticity[97,185–187]. Moreover, synthetic matrices can be spatially patterned to controllably release growth factor and/or induce matrix stiffness or viscoelasticity changes to guide symmetry breaking, pattern formation and morphogenesis of embryo models[134,188] (Fig. 4b). For example, a photo-induced hydrogel cross-link exchange reaction was used to spatiotemporally alter the local viscoelasticity of a synthetic hydrogel formed through reaction between PEG-dibenzylcyclooctyne and allyl sulfide bis(PEG3-azide)[189]. This system enabled control of epithelial tissue curvatures and the study of how these influence mechanotransduction pathways to instruct crypt morphogenesis in intestinal organoids[189]. The spatiotemporal control of extracellular signals, offered by such synthetic hydrogels, offers another layer of regulation that can be integrated with other bioengineering approaches, such as microfluidics and optogenetics, to develop controllable and programmable embryo models.

Synthetic biology for embryo models

Synthetic biology tools enable control of transcription factor expression, modulation of signalling pathways, manipulation of epigenetic modifications, directing cell fate specification and regulation of cell adhesion[190–193]. Thus, orthogonal to microfluidics, micropatterning and synthetic biomaterials, synthetic biology can be leveraged to achieve programmable cellular complexity, architecture and function in bioengineered embryo and organ models (Fig. 5).

Engineering cell fate

Overexpression of transcription factors through genetic engineering has been commonly used to induce cell differentiation or transdifferentiation (Fig. 5a). Compared with chemical induction, overexpression of transcription factors can produce specific cell lineages more quickly and efficiently, and likely with greater homogeneity. ETX embryo models resemble the mouse egg cylinder; however, they cannot develop further beyond the onset of gastrulation[67,68] likely due to heterogeneous TSC and XEN (sub)populations[71,194] (Table 1). Replacing mouse TSCs and XENs with mouse ES cells transiently overexpressing *Cdx2* and *Gata4*, respectively, led to mouse embryo models to develop beyond gastrulation and reach early organogenesis stages[70–72], albeit with a low efficiency (<1%) and containing organ primordia with structural defects (Table 1). Similar transcription factor overexpression strategies were used to generate extra-embryonic lineages before assembling them with either naive or primed hPS cells for constructing peri-implantation human embryo models[81,82,84–87] (Table 1).

Genetic engineering tools can also be combined with 3D bioprinting to generate organoids with controlled cellular composition and organization. Specifically, an orthogonally induced differentiation method was developed to generate endothelial cells and neurons by overexpressing *ETV2* and *NGN1*, respectively, in the same hPS cell population independently of culture medium conditions[195]. This method was used to generate vascularized cortical organoids[195]. Moreover, integrating orthogonally induced differentiation with multi-material bioprinting of hPS cells with inducible transcription factor overexpression generated patterned neural tissues with layered regions composed of neural stem cells, endothelium and neurons[195].

Engineering cell adhesion

Cell–cell adhesions influence tissue development by regulating tissue architecture, cell behaviour and signalling processes. For example,

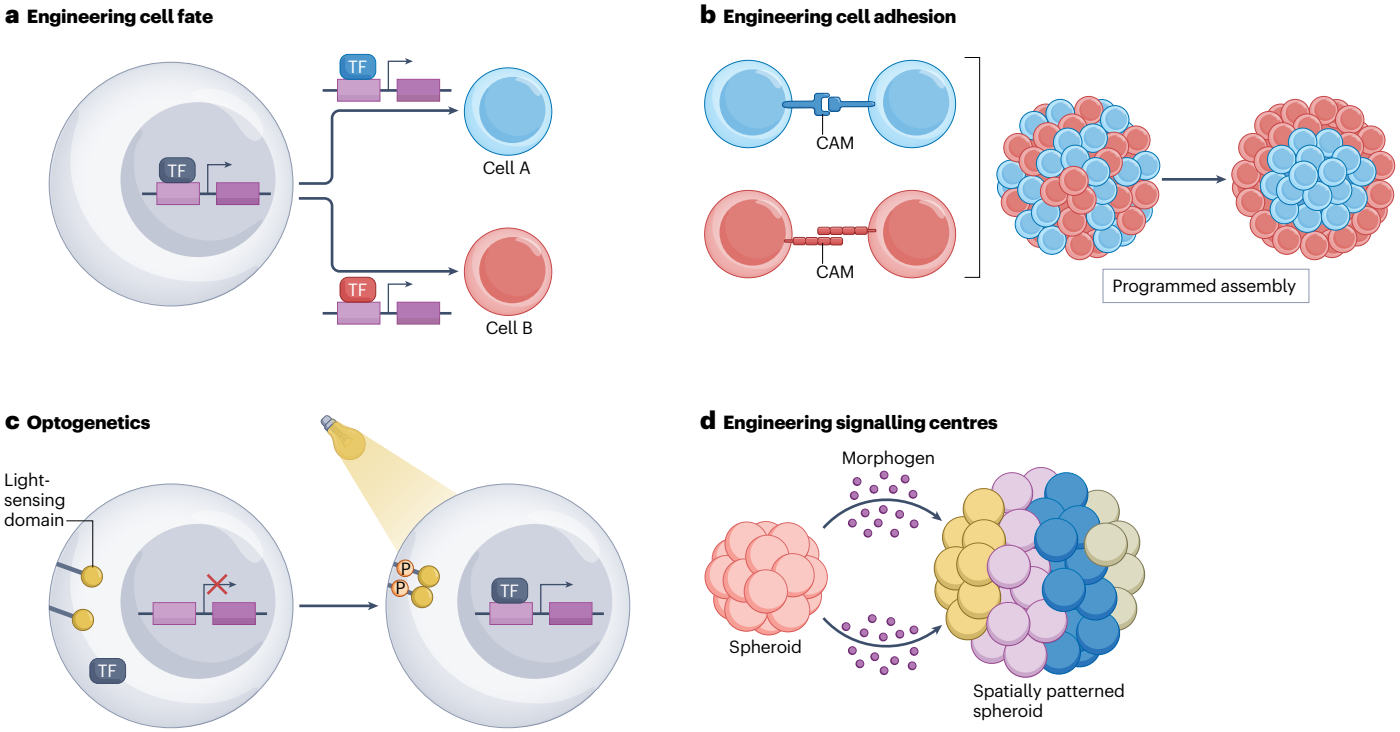


Fig. 5 | Engineering cell behaviours using synthetic biology. a, Engineering cell fate by controlling transcription factor (TF) expression to produce specific cell lineages. **b**, Engineering cell adhesion using synthetic receptors, enabling programmed generation of spatially patterned multicellular structures[199]. **c**, Optogenetics to modulate intracellular signalling pathways, for example, by fusing a light-sensing domain with ligand receptors. **d**, Engineering signalling centres to regulate fate specification and tissue patterning. Localized signalling centres can be generated by genetically engineering cells to express signalling molecules, which will guide spatial patterning of adjacent spheroids. Different colours represent different cell types. CAM, cell-adhesion molecule.

cadherins form adherens junctions between adjacent cells contribute to tissue morphogenesis by maintaining tissue integrity, shape and organization[196,197]. Varying the expression levels and types of cadherins could result in autonomous cell sorting and segregation during tissue development, a phenomenon termed differential adhesion[197]. This process is essential in establishing tissue boundaries and spatial organization during development[196,197]. Interestingly, overexpressing cadherin molecules specific to the mouse EPI and trophectoderm in mouse ES cells and mouse TSCs, respectively, improved the efficiency of ETX embryo model generation by almost threefold through autonomous cell sorting and segregation similar to those in mouse blastocyst formation[198].

Since the early 2000s, synthetic biologists have repurposed physical elements and concepts from natural receptors to engineer synthetic receptors[190]. These technologies implement customized sense-and-respond programmes that link interactions of a cell with extracellular and intracellular cues to user-defined responses, including rationally programmed assembly of multicellular architectures[192,199] (Fig. 5b). Over the years, the library of synthetic receptors and their capabilities has substantially evolved. For example, synthetic cell-adhesion molecules were demonstrated by combining orthogonal extracellular interactions with intracellular domains from native adhesion molecules such as cadherins and integrins[199]. These molecules yield customized cell–cell interactions with adhesion properties similar to native interactions, including eliciting intracellular actin cytoskeleton dynamics and tension[199]. How synthetic receptors could be used to improve the efficiency of embryo and organ models remains to be demonstrated.

Outlook

Bioengineering strategies can be used to engineer pattern formation and morphogenesis to generate advanced embryo models with improved efficiency, tuneability, cellular complexity, composition and organization. The heterogeneity of initial stem cell populations and their less characterized functions should also be considered. To this end, synthetic biology approaches to engineer cell fate can provide more uniform cell sources to generate embryo models.

Stringent validation of these models is essential for downstream applications. However, it remains challenging to compare embryo models with in vivo embryos of the same species and compatible stages, especially for human ones. In vivo and ex vivo cultures of human and non-human primate embryos provide important molecular and cellular information for authenticating and benchmarking human embryo models[200–207]. Single-cell multiomics, including single-cell RNA sequencing, provides a wealth of information about the molecular characteristics and functions of single cells as well as insights on cellular heterogeneity, cell–cell variability and complex biological processes. Several data sets have been generated from in vivo and ex vivo cultured human and non-human primate embryos at different development stages, which could be used as references in embryo modelling[204–207]. Importantly, not only molecular signatures, cell lineage identities or multicellular tissue organization at isolated time

Box 2 | Ethical considerations

The similarity of stem cell-based embryo models to natural embryos, especially human ones, raises ethical concerns. In most countries, stem cell-based embryo models currently do not explicitly fit into existing legal regulatory categories. Historically, scientific societies such as the International Society for Stem Cell Research have contributed in establishing ethical frameworks for stem cell research and provided updated ethical guidelines for stem cell research in 2021 (ref. 210), which included considerations on embryo modelling research. The International Society for Stem Cell Research proposed that integrated embryo models should require stricter oversight than non-integrated ones as well as prohibiting the transfer of human embryo models into any uterus or the use of human embryo models for reproduction purposes. Although none of the current embryo models is considered equivalent to human embryos or has shown potential to develop into a fetus, as the field progresses, they may mimic the entire natural embryo, or a considerable portion thereof, more closely in terms of molecular signatures, tissue structures and development potential. There are ongoing discussions on the legal definition of human embryos and at what point human embryo models should be regulated as natural ones[209,212,213]. Ideally, the least ethically challenging models should be used whenever possible; for example, although studying how the whole embryo develops might require integrated models, studies of individual germ layer development or the formation of specific organs might not need them. Several non-integrated embryo models can mimic at least some aspects of human development, including gastrulation and early organ formation[25,31,136,143,174,175]. These models are easier to study because they contain clearly defined cell types organized into regular patterns, unlike their integrated counterpart. Moreover, because non-integrated embryo models are often built using bioengineering tools, they are more efficient, reproducible and scalable.

points should be compared but the dynamic and progressive tissue developmental events that cultivate their morphology, architecture and function must also be considered.

Ethical challenges still remain, with ongoing discussions about regulating human embryo models; in particular, integrated systems should follow regulations similar to those for natural human embryos[208–210] (Box 2). Thus, it is desirable to choose less ethically challenging embryo models whenever possible. Embryo models should be purposely selected; the specific developmental stages and corresponding cell lineage developments that each embryo model can recapitulate (for example, embryonic or extra-embryonic lineages, or integrated versus non-integrated models) must be considered when examining its usefulness for specific applications. Increased cellular complexity and composition often comes with decreased tissue organization and/or model controllability and reproducibility. For example, studies of individual germ layer development likely do not need the use of integrated embryo models that contain certain extra-embryonic cell lineages. By contrast, investigating tissue–tissue interactions, such as those between embryonic and extra-embryonic lineages, require more complex models that contain all relevant cell types[81–87]. For fundamental mechanistic studies, embryo models that closely resemble in vivo development in terms of lineage diversification, tissue patterning, morphogenetic events and tissue architecture are desired (such as the 3D neural folding model[136]). For high-content screening and other translational applications, models with high reproducibility and scalability are preferred (such as 2D micropatterned neural rosette arrays[162]).

The field of stem cell-based embryo models is progressing rapidly, with tremendous potential for both fundamental and translational applications. As the field moves forward, social responsibility, transparency and effective engagement with all stakeholders (including the public) will be essential to ensure a smooth and rapid progress.

Published online: 08 October 2024

References

1. Wolpert, L., Tickle, C. & Arias, A. M. *Principles of Development* (Oxford University Press, 2015).
2. Simunovic, M. & Brivanlou, A. H. Embryoids, organoids and gastruloids: new approaches to understanding embryogenesis. *Development* **144**, 976–985 (2017).
3. Fu, J., Warmflash, A. & Lutolf, M. P. Stem-cell-based embryo models for fundamental research and translation. *Nat. Mater.* **20**, 132–144 (2021).
4. Rossant, J. & Tam, P. P. L. Opportunities and challenges with stem cell-based embryo models. *Stem Cell Rep.* **16**, 1031–1038 (2021).
5. Shahbazi, M. N., Siggia, E. D. & Zernicka-Goetz, M. Self-organization of stem cells into embryos: a window on early mammalian development. *Science* **364**, 948–951 (2019).
6. Keller, G. Embryonic stem cell differentiation: emergence of a new era in biology and medicine. *Genes Dev.* **19**, 1129–1155 (2005).
7. Sasai, Y. Cytosystems dynamics in self-organization of tissue architecture. *Nature* **493**, 318–326 (2013).
8. Turner, D. A., Baillie-Johnson, P. & Martinez Arias, A. Organoids and the genetically encoded self-assembly of embryonic stem cells. *BioEssays* **38**, 181–191 (2016).
9. Terhune, A. H., Bok, J., Sun, S. & Fu, J. Stem cell-based models of early mammalian development. *Development* **149**, dev201015 (2022).
10. Moris, N., Alev, C., Pera, M. & Martinez Arias, A. Biomedical and societal impacts of in vitro embryo models of mammalian development. *Stem Cell Rep.* **16**, 1021–1030 (2021).
11. Rossant, J. Why study human embryo development? *Dev. Biol.* **509**, 43–50 (2024).
12. Balázsi, G., van Oudenaarden, A. & Collins, J. J. Cellular decision making and biological noise: from microbes to mammals. *Cell* **144**, 910–925 (2011).
13. Shao, Y. & Fu, J. Engineering multiscale structural orders for high-fidelity embryoids and organoids. *Cell Stem Cell* **29**, 722–743 (2022).
14. Tanaka, S., Kunath, T., Hadjantonakis, A.-K., Nagy, A. & Rossant, J. Promotion of trophoblast stem cell proliferation by FGF4. *Science* **282**, 2072–2075 (1998).
15. Okae, H. et al. Derivation of human trophoblast stem cells. *Cell Stem Cell* **22**, 50–63.e6 (2018).
16. Kunath, T. et al. Imprinted X-inactivation in extra-embryonic endoderm cell lines from mouse blastocysts. *Development* **132**, 1649–1661 (2005).
17. Du, P. & Wu, J. Hallmarks of totipotent and pluripotent stem cell states. *Cell Stem Cell* **31**, 312–333 (2024).
18. Salazar-Ciudad, I., Jernvall, J. & Newman, S. A. Mechanisms of pattern formation in development and evolution. *Development* **130**, 2027–2037 (2003).
19. Schweisguth, F. & Corson, F. Self-organization in pattern formation. *Dev. Cell* **49**, 659–677 (2019).
20. Simsek, M. F. & Özbudak, E. M. Patterning principles of morphogen gradients. *Open Biol.* **12**, 220224 (2022).
21. Turing, A. M. The chemical basis of morphogenesis. *Bull. Math. Biol.* **52**, 153–197 (1990).
22. Sick, S., Reinker, S., Timmer, J. & Schlake, T. WNT and DKK determine hair follicle spacing through a reaction-diffusion mechanism. *Science* **314**, 1447–1450 (2006).
23. Etoc, F. et al. A balance between secreted inhibitors and edge sensing controls gastruloid self-organization. *Dev. Cell* **39**, 302–315 (2016).
24. Kagawa, H. et al. Human blastoids model blastocyst development and implantation. *Nature* **601**, 600–605 (2022).
25. Warmflash, A., Sorre, B., Etoc, F., Siggia, E. D. & Brivanlou, A. H. A method to recapitulate early embryonic spatial patterning in human embryonic stem cells. *Nat. Methods* **11**, 847–854 (2014).
26. Wolpert, L. Positional information and pattern formation. *Curr. Top. Dev. Biol.* **117**, 597–608 (2016).
27. Sun, S., Xue, X. & Fu, J. Modeling development using microfluidics: bridging gaps to foster fundamental and translational research. *Curr. Opin. Genet. Dev.* **82**, 102097 (2023).
28. Xu, P.-F. et al. Construction of a mammalian embryo model from stem cells organized by a morphogen signalling centre. *Nat. Commun.* **12**, 3277 (2021).
29. Zheng, Y. et al. Controlled modelling of human epiblast and amnion development using stem cells. *Nature* **573**, 421–425 (2019).
This article reports a microfluidics-based human embryo model that recapitulates key landmarks during human peri-implantation development.

30. Rifes, P. et al. Modeling neural tube development by differentiation of human embryonic stem cells in a microfluidic WNT gradient. *Nat. Biotechnol.* **38**, 1265–1273 (2020).
31. Xue, X. et al. A patterned human neural tube model using microfluidic gradients. *Nature* **628**, 391–399 (2024).
Refs. 30 and 31 describe the successful application of microfluidic gradient devices for building advanced human neural tube development models with proper axial patterning.
32. Morales, J. S., Raspopovic, J. & Marcon, L. From embryos to embryoids: how external signals and self-organization drive embryonic development. *Stem Cell Rep.* **16**, 1039–1050 (2021).
33. Rossant, J. & Tam, P. P. L. Blastocyst lineage formation, early embryonic asymmetries and axis patterning in the mouse. *Development* **136**, 701–713 (2009).
34. Wennekamp, S., Mesecke, S., Nédélec, F. & Hiiragi, T. A self-organization framework for symmetry breaking in the mammalian embryo. *Nat. Rev. Mol. Cell Biol.* **14**, 452–459 (2013).
35. Maître, J.-L., Niwayama, R., Turlier, H., Nédélec, F. & Hiiragi, T. Pulsatile cell-autonomous contractility drives compaction in the mouse embryo. *Nat. Cell Biol.* **17**, 849–855 (2015).
36. Fleming, T. P., Cannon, P. M. & Pickering, S. J. The cytoskeleton, endocytosis and cell polarity in the mouse preimplantation embryo. *Dev. Biol.* **113**, 406–419 (1986).
37. Wicklow, E. et al. HIPPO pathway members restrict SOX2 to the inner cell mass where it promotes ICM fates in the mouse blastocyst. *PLoS Genet.* **10**, e1004618 (2014).
38. Nishioka, N. et al. The Hippo signaling pathway components Lats and Yap pattern Tead4 activity to distinguish mouse trophectoderm from inner cell mass. *Dev. Cell* **16**, 398–410 (2009).
39. Maître, J.-L. et al. Asymmetric division of contractile domains couples cell positioning and fate specification. *Nature* **536**, 344–348 (2016).
40. Korotkevich, E. et al. The apical domain is required and sufficient for the first lineage segregation in the mouse embryo. *Dev. Cell* **40**, 235–247.e7 (2017).
41. Niwayama, R. et al. A tug-of-war between cell shape and polarity controls division orientation to ensure robust patterning in the mouse blastocyst. *Dev. Cell* **51**, 564–574.e6 (2019).
42. Barcroft, L. C., Offenberg, H., Thomsen, P. & Watson, A. J. Aquaporin proteins in murine trophectoderm mediate transepithelial water movements during cavitation. *Dev. Biol.* **256**, 342–354 (2003).
43. Dumortier, J. G. et al. Hydraulic fracturing and active coarsening position the lumen of the mouse blastocyst. *Science* **365**, 465–468 (2019).
44. Kang, M., Garg, V. & Hadjantonakis, A.-K. Lineage establishment and progression within the inner cell mass of the mouse blastocyst requires FGFR1 and FGFR2. *Dev. Cell* **41**, 496–510.e5 (2017).
45. Saiz, N., Grabarek, J. B., Sabherwal, N., Papalopulu, N. & Plusa, B. Atypical protein kinase C couples cell sorting with primitive endoderm maturation in the mouse blastocyst. *Development* **140**, 4311–4322 (2013).
46. Kuijk, E. W. et al. The roles of FGF and MAP kinase signaling in the segregation of the epiblast and hypoblast cell lineages in bovine and human embryos. *Development* **139**, 871–882 (2012).
47. Roode, M. et al. Human hypoblast formation is not dependent on FGF signalling. *Dev. Biol.* **361**, 358–363 (2012).
48. Linneberg-Agerholm, M. et al. Naïve human pluripotent stem cells respond to Wnt, Nodal and LIF signalling to produce expandable naïve extra-embryonic endoderm. *Development* **146**, dev180620 (2019).
49. Dattani, A. et al. Naive pluripotent stem cell-based models capture FGF-dependent human hypoblast lineage specification. *Cell Stem Cell* **31**, 1058–1071.e5 (2024).
50. Rivron, N. C. et al. Blastocyst-like structures generated solely from stem cells. *Nature* **557**, 106–111 (2018).
51. Sozen, B. et al. Self-organization of mouse stem cells into an extended potential blastoid. *Dev. Cell* **51**, 698–712.e8 (2019).
52. Li, R. et al. Generation of blastocyst-like structures from mouse embryonic and adult cell cultures. *Cell* **179**, 687–702.e18 (2019).
53. Liu, X. et al. Modelling human blastocysts by reprogramming fibroblasts into iBlastoids. *Nature* **591**, 627–632 (2021).
54. Yanagida, A. et al. Naive stem cell blastocyst model captures human embryo lineage segregation. *Cell Stem Cell* **28**, 1016–1022.e4 (2021).
55. Yu, L. et al. Blastocyst-like structures generated from human pluripotent stem cells. *Nature* **591**, 620–626 (2021).
56. Yu, L. et al. Large-scale production of human blastoids amenable to modeling blastocyst development and maternal-fetal cross talk. *Cell Stem Cell* **30**, 1246–1261.e9 (2023).
57. Sozen, B. et al. Reconstructing aspects of human embryogenesis with pluripotent stem cells. *Nat. Commun.* **12**, 5550 (2021).
58. Shibata, S. et al. Modeling embryo-endometrial interface recapitulating human embryo implantation. *Sci. Adv.* **10**, eadi4819 (2024).
This article reports feto-maternal assembloids by co-culturing endometrial organoids with blastoids to recapitulate critical events during implantation, including apposition, adhesion and invasion.
59. Rodriguez, T. A., Srinivas, S., Clements, M. P., Smith, J. C. & Beddington, R. S. P. Induction and migration of the anterior visceral endoderm is regulated by the extra-embryonic ectoderm. *Development* **132**, 2513–2520 (2005).
60. Yamamoto, M. et al. Antagonism between Smad1 and Smad2 signaling determines the site of distal visceral endoderm formation in the mouse embryo. *J. Cell Biol.* **184**, 323–334 (2009).
61. Yamamoto, M. et al. Nodal antagonists regulate formation of the anteroposterior axis of the mouse embryo. *Nature* **428**, 387–392 (2004).
62. Belo, J. A. et al. Cerberus-like is a secreted factor with neuralizing activity expressed in the anterior primitive endoderm of the mouse gastrula. *Mech. Dev.* **68**, 45–57 (1997).
63. Kemp, C. R. et al. Expression of Frizzled5, Frizzled7, and Frizzled10 during early mouse development and interactions with canonical Wnt signaling. *Dev. Dyn.* **236**, 2011–2019 (2007).
64. Rossant, J. & Tam, P. P. L. Early human embryonic development: blastocyst formation to gastrulation. *Dev. Cell* **57**, 152–165 (2022).
65. Molè, M. A. et al. A single cell characterisation of human embryogenesis identifies pluripotency transitions and putative anterior hypoblast centre. *Nat. Commun.* **12**, 3679 (2021).
66. Zhu, Q. et al. Decoding anterior-posterior axis emergence among mouse, monkey, and human embryos. *Dev. Cell* **58**, 63–79.e4 (2023).
67. Harrison, S. E., Sozen, B., Christodoulou, N., Kyprianou, C. & Zernicka-Goetz, M. Assembly of embryonic and extraembryonic stem cells to mimic embryogenesis in vitro. *Science* **356**, eaal1810 (2017).
68. Sozen, B. et al. Self-assembly of embryonic and two extra-embryonic stem cell types into gastrulating embryo-like structures. *Nat. Cell Biol.* **20**, 979–989 (2018).
69. Zhang, S. et al. Implantation initiation of self-assembled embryo-like structures generated using three types of mouse blastocyst-derived stem cells. *Nat. Commun.* **10**, 496 (2019).
70. Amadei, G. et al. Embryo model completes gastrulation to neurulation and organogenesis. *Nature* **610**, 143–153 (2022).
71. Tarazi, S. et al. Post-gastrulation synthetic embryos generated ex utero from mouse naive ESCs. *Cell* **185**, 3290–3306.e25 (2022).
72. Lau, K. Y. C. et al. Mouse embryo model derived exclusively from embryonic stem cells undergoes neurulation and heart development. *Cell Stem Cell* **29**, 1445–1458.e8 (2022).
73. Aguilera-Castrejon, A. et al. Ex utero mouse embryogenesis from pre-gastrulation to late organogenesis. *Nature* **593**, 119–124 (2021).
74. Girgin, M. U. et al. Bioengineered embryoids mimic post-implantation development in vitro. *Nat. Commun.* **12**, 5140 (2021).
75. Birey, F. et al. Assembly of functionally integrated human forebrain spheroids. *Nature* **545**, 54–59 (2017).
76. Koike, H. et al. Modelling human hepato-biliary-pancreatic organogenesis from the foregut–midgut boundary. *Nature* **574**, 112–116 (2019).
77. Simunovic, M. et al. A 3D model of a human epiblast reveals BMP4-driven symmetry breaking. *Nat. Cell Biol.* **21**, 900–910 (2019).
78. Simunovic, M., Siggia, E. D. & Brivanlou, A. H. In vitro attachment and symmetry breaking of a human embryo model assembled from primed embryonic stem cells. *Cell Stem Cell* **29**, 962–972.e4 (2022).
79. Shao, Y. et al. A pluripotent stem cell-based model for post-implantation human amniotic sac development. *Nat. Commun.* **8**, 208 (2017).
80. Yang, R. et al. Amnion signals are essential for mesoderm formation in primates. *Nat. Commun.* **12**, 5126 (2021).
81. Karvas, R. M. et al. 3D-cultured blastoids model human embryogenesis from pre-implantation to early gastrulation stages. *Cell Stem Cell* **30**, 1148–1165.e7 (2023).
82. Hislop, J. et al. Modelling post-implantation human development to yolk sac blood emergence. *Nature* **626**, 367–376 (2023).
83. Liu, L. et al. Modeling post-implantation stages of human development into early organogenesis with stem-cell-derived peri-gastruloids. *Cell* **186**, 3776–3792.e16 (2023).
84. Oldak, B. et al. Complete human day 14 post-implantation embryo models from naive ES cells. *Nature* **622**, 562–573 (2023).
85. Pedroza, M. et al. Self-patterning of human stem cells into post-implantation lineages. *Nature* **622**, 574–583 (2023).
86. Weatherbee, B. A. T. et al. Pluripotent stem cell-derived model of the post-implantation human embryo. *Nature* **622**, 584–593 (2023).
87. Okubo, T. et al. Hypoblast from human pluripotent stem cells regulates epiblast development. *Nature* **626**, 357–366 (2024).
88. Storey, K. G. et al. Early posterior neural tissue is induced by FGF in the chick embryo. *Development* **125**, 473–484 (1998).
89. Niederreither, K., Subbarayan, V., Dollé, P. & Chambon, P. Embryonic retinoic acid synthesis is essential for early mouse post-implantation development. *Nat. Genet.* **21**, 444–448 (1999).
90. Nordström, U., Jessell, T. M. & Edlund, T. Progressive induction of caudal neural character by graded Wnt signaling. *Nat. Neurosci.* **5**, 525–532 (2002).
91. Wurst, W. & Bally-Cuif, L. Neural plate patterning: upstream and downstream of the isthmic organizer. *Nat. Rev. Neurosci.* **2**, 99–108 (2001).
92. Sagner, A. & Briscoe, J. Establishing neuronal diversity in the spinal cord: a time and a place. *Development* **146**, dev182154 (2019).
93. Wilson, S. W. & Rubenstein, J. L. R. Induction and dorsoventral patterning of the telencephalon. *Neuron* **28**, 641–651 (2000).
94. Wilson, L., Gale, E., Chambers, D. & Maden, M. Retinoic acid and the control of dorsoventral patterning in the avian spinal cord. *Dev. Biol.* **269**, 433–446 (2004).
95. Meinhardt, A. et al. 3D reconstitution of the patterned neural tube from embryonic stem cells. *Stem Cell Rep.* **3**, 987–999 (2014).
96. Zheng, Y. et al. Dorsal-ventral patterned neural cyst from human pluripotent stem cells in a neurogenic niche. *Sci. Adv.* **5**, eaax5933 (2019).

97. Ranga, A. et al. Neural tube morphogenesis in synthetic 3D microenvironments. *Proc. Natl Acad. Sci.* **113**, E6831–E6839 (2016).
98. Abdel Fattah, A. R., Grebenyuk, S., de Rooij, L. P. M. H., Salmon, I. & Ranga, A. Neuroepithelial organoid patterning is mediated by a neighborhood watch mechanism. *Cell Rep.* **42**, 113334 (2023).
99. Krammer, T. et al. Mouse neural tube organoids self-organize floorplate through BMP-mediated cluster competition. *Dev. Cell* **59**, 1940–1953.e10 (2024).
100. Pavon, N. et al. Patterning ganglionic eminences in developing human brain organoids using a morphogen-gradient-inducing device. *Cell Rep. Methods* **4**, 100689 (2024).
101. Gjorevski, N. et al. Tissue geometry drives deterministic organoid patterning. *Science* **375**, eaaw9021 (2022).
This article reports bioengineering strategies to specify the initial geometry of intestinal organoids, which in turn controls their spatial patterning and crypt formation.
102. Nikolaev, M. et al. Homeostatic mini-intestines through scaffold-guided organoid morphogenesis. *Nature* **585**, 574–578 (2020).
103. Rodriguez, N. M., Desai, R. A., Trappmann, B., Baker, B. M. & Chen, C. S. Micropatterned multicolor dynamically adhesive substrates to control cell adhesion and multicellular organization. *Langmuir* **30**, 1327–1335 (2014).
104. Wright, D., Rajalingam, B., Selvarasah, S., Dokmeci, M. R. & Khademhosseini, A. Generation of static and dynamic patterned co-cultures using microfabricated parylene-C stencils. *Lab. Chip* **7**, 1272–1279 (2007).
105. March, S. et al. Micropatterned coculture of primary human hepatocytes and supportive cells for the study of hepatotropic pathogens. *Nat. Protoc.* **10**, 2027–2053 (2015).
106. Li, C. Y. et al. Micropatterned cell-cell interactions enable functional encapsulation of primary hepatocytes in hydrogel microtissues. *Tissue Eng. Part. A* **20**, 2200–2212 (2014).
107. Hui, E. E. & Bhatia, S. N. Micromechanical control of cell–cell interactions. *Proc. Natl Acad. Sci. USA* **104**, 5722–5726 (2007).
108. Manfrin, A. et al. Engineered signaling centers for the spatially controlled patterning of human pluripotent stem cells. *Nat. Methods* **16**, 640–648 (2019).
109. Xue, X. et al. Mechanics-guided embryonic patterning of neuroectoderm tissue from human pluripotent stem cells. *Nat. Mater.* **17**, 633–641 (2018).
110. Khadir, Z. et al. Surface micropatterning for the formation of an in vitro functional endothelial model for cell-based biosensors. *Biosens. Bioelectron.* **214**, 114481 (2022).
111. Murphy, S. V. & Atala, A. 3D bioprinting of tissues and organs. *Nat. Biotechnol.* **32**, 773–785 (2014).
112. Banerjee, D. et al. Strategies for 3D bioprinting of spheroids: a comprehensive review. *Biomaterials* **291**, 121881 (2022).
113. Daly, A. C., Davidson, M. D. & Burdick, J. A. 3D bioprinting of high cell-density heterogeneous tissue models through spheroid fusion within self-healing hydrogels. *Nat. Commun.* **12**, 753 (2021).
114. Roth, J. G. et al. Spatially controlled construction of assembloids using bioprinting. *Nat. Commun.* **14**, 4346 (2023).
115. Skylar-Scott, M. A. et al. Biomanufacturing of organ-specific tissues with high cellular density and embedded vascular channels. *Sci. Adv.* **5**, eaaw2459 (2019).
116. Ben-Reuven, L. & Reiner, O. Toward spatial identities in human brain organoids-on-chip induced by morphogen-soaked beads. *Bioengineering* **7**, 164 (2020).
117. Marín-Llera, J. C. & Chimal-Monroy, J. Analysis of cell differentiation, morphogenesis, and patterning during chicken embryogenesis using the soaked-bead assay. *J. Vis. Exp.* https://doi.org/10.3791/63187 (2022).
118. Bonner, M. G., Gudapati, H., Mou, X. & Musah, S. Microfluidic systems for modeling human development. *Development* **149**, dev199463 (2022).
119. Sonnen, K. F. & Merten, C. A. Microfluidics as an emerging precision tool in developmental biology. *Dev. Cell* **48**, 293–311 (2019).
120. Cederquist, G. Y. et al. Specification of positional identity in forebrain organoids. *Nat. Biotechnol.* **37**, 436–444 (2019).
This article describes a method to induce spatial patterning in human forebrain organoids by assembling them with a cluster of genetically modified, SHH-secreting hPS cells that serve as a signalling centre.
121. Toda, S. et al. Engineering synthetic morphogen systems that can program multicellular patterning. *Science* **370**, 327–331 (2020).
122. Legnini, I. et al. Spatiotemporal, optogenetic control of gene expression in organoids. *Nat. Methods* **20**, 1544–1552 (2023).
This article describes a system that enables light-inducible activation and repression of target genes in programmable spatiotemporal patterns, which is further utilized to locally activate SHH signalling in spinal cord organoids to induce ventral patterning.
123. Martínez-Ara, G. et al. Optogenetic control of apical constriction induces synthetic morphogenesis in mammalian tissues. *Nat. Commun.* **13**, 5400 (2022).
124. Gurdon, J. B., Harger, P., Mitchell, A. & Lemaire, P. Activin signalling and response to a morphogen gradient. *Nature* **371**, 487–492 (1994).
125. Gurdon, J., Mitchell, A. & Mahony, D. Direct and continuous assessment by cells of their position in a morphogen gradient. *Nature* **376**, 520–521 (1995).
126. Reyes, D. R. et al. Accelerating innovation and commercialization through standardization of microfluidic-based medical devices. *Lab. Chip* **21**, 9–21 (2021).
127. Repina, N. A. et al. Optogenetic control of Wnt signaling models cell-intrinsic embryogenic patterning using 2D human pluripotent stem cell culture. *Development* **150**, dev201386 (2023).
128. De Santis, R., Etoc, F., Rosado-Olivieri, E. A. & Brivanlou, A. H. Self-organization of human dorsal-ventral forebrain structures by light induced SHH. *Nat. Commun.* **12**, 6768 (2021).
129. Emiliani, V. et al. Optogenetics for light control of biological systems. *Nat. Rev. Methods Primers* **2**, 55 (2022).
130. Sheng, G., Martinez Arias, A. & Sutherland, A. The primitive streak and cellular principles of building an amniote body through gastrulation. *Science* **374**, abg1727 (2021).
131. Miao, Y. & Pourquié, O. Cellular and molecular control of vertebrate somitogenesis. *Nat. Rev. Mol. Cell Biol.* **25**, 517–533 (2024).
132. Nikolopoulou, E., Galea, G. L., Rolo, A., Greene, N. D. E. & Copp, A. J. Neural tube closure: cellular, molecular and biomechanical mechanisms. *Development* **144**, 552–566 (2017).
133. Walma, D. A. C. & Yamada, K. M. The extracellular matrix in development. *Development* **147**, dev175596 (2020).
134. Kratochvil, M. J. et al. Engineered materials for organoid systems. *Nat. Rev. Mater.* **4**, 606–622 (2019).
135. van den Brink, S. C. et al. Single-cell and spatial transcriptomics reveal somitogenesis in gastruloids. *Nature* **582**, 405–409 (2020).
136. Karzbrun, E. et al. Human neural tube morphogenesis in vitro by geometric constraints. *Nature* **599**, 268–272 (2021).
This article reports a hPS cell-based neural tube folding model by combining micropatterning and 3D culture.
137. Veenvliet, J. V. et al. Mouse embryonic stem cells self-organize into trunk-like structures with neural tube and somites. *Science* **370**, eaba4937 (2020).
138. Steventon, B., Busby, L. & Arias, A. M. Establishment of the vertebrate body plan: rethinking gastrulation through stem cell models of early embryogenesis. *Dev. Cell* **56**, 2405–2418 (2021).
139. Tewary, M. et al. A stepwise model of reaction-diffusion and positional information governs self-organized human peri-gastrulation-like patterning. *Development* **144**, 4298–4312 (2017).
140. Heemskerk, I. et al. Rapid changes in morphogen concentration control self-organized patterning in human embryonic stem cells. *eLife* **8**, e40526 (2019).
141. Zhang, Z., Zwick, S., Loew, E., Grimley, J. S. & Ramanathan, S. Mouse embryo geometry drives formation of robust signaling gradients through receptor localization. *Nat. Commun.* **10**, 4516 (2019).
142. Beccari, L. et al. Multi-axial self-organization properties of mouse embryonic stem cells into gastruloids. *Nature* **562**, 272–276 (2018).
143. Moris, N. et al. An in vitro model of early anteroposterior organization during human development. *Nature* **582**, 410–415 (2020).
144. Sullivan, A. E. & Santos, S. D. M. The ever-growing world of gastruloids: autogenous models of mammalian embryogenesis. *Curr. Opin. Genet. Dev.* **82**, 102102 (2023).
145. Rossi, G. et al. Capturing cardiogenesis in gastruloids. *Cell Stem Cell* **28**, 230–240.e6 (2021).
146. Vianello, S. & Lutolf, M. P. In vitro endoderm emergence and self-organisation in the absence of extraembryonic tissues and embryonic architecture. Preprint at *bioRxiv* https://doi.org/10.1101/2020.06.07.138883 (2021).
147. Sozen, B., Conkar, D. & Veenvliet, J. V. Carnegie in 4D? Stem-cell-based models of human embryo development. *Semin. Cell Dev. Biol.* **131**, 44–57 (2022).
148. Muncie, J. M. et al. Mechanical tension promotes formation of gastrulation-like nodes and patterns mesoderm specification in human embryonic stem cells. *Dev. Cell* **55**, 679–694.e11 (2020).
This article presents a hPS cell-based model that recapitulates gastrulation-like morphogenesis by culturing micropatterned hPS cell colonies on soft hydrogels, where tissue geometries dictate the formation of 'gastrulation-like' nodes in regions of high cell-adhesion tension by promoting WNT signalling and mesoderm specification.
149. Caldarelli, P., Chamolly, A., Alegria-Prévot, O., Gros, J. & Corson, F. Self-organized tissue mechanics underlie embryonic regulation. Preprint at *bioRxiv* https://doi.org/10.1101/2021.10.08.463661 (2021).
150. Brunet, T. et al. Evolutionary conservation of early mesoderm specification by mechanotransduction in *Bilateria*. *Nat. Commun.* **4**, 2821 (2013).
151. Tzouanacou, E., Wegener, A., Wymeersch, F. J., Wilson, V. & Nicolas, J.-F. Redefining the progression of lineage segregations during mammalian embryogenesis by clonal analysis. *Dev. Cell* **17**, 365–376 (2009).
152. Underhill, E. J. & Toettcher, J. E. Control of gastruloid patterning and morphogenesis by the Erk and Akt signaling pathways. *Development* **150**, dev201663 (2023).
153. de Jong, M. A. et al. The shapes of elongating gastruloids are consistent with convergent extension driven by a combination of active cell crawling and differential adhesion. *PLOS Comput. Biol.* **20**, e1011825 (2024).
154. Sutherland, A., Keller, R. & Lesko, A. Convergent extension in mammalian morphogenesis. *Semin. Cell Dev. Biol.* **100**, 199–211 (2020).
155. Morriss-Kay, G. & Tuckett, F. The role of microfilaments in cranial neurulation in rat embryos: effects of short-term exposure to cytochalasin D. *Development* **88**, 333–348 (1985).
156. Ybot-Gonzalez, P. & Copp, A. J. Bending of the neural plate during mouse spinal neurulation is independent of actin microfilaments. *Dev. Dyn.* **215**, 273–283 (1999).
157. Gurniak, C. B., Perlas, E. & Witke, W. The actin depolymerizing factor n-cofilin is essential for neural tube morphogenesis and neural crest cell migration. *Dev. Biol.* **278**, 231–241 (2005).
158. Greene, N. D. E. & Copp, A. J. Neural tube defects. *Annu. Rev. Neurosci.* **37**, 221–242 (2014).
159. Moon, L. D. & Xiong, F. Mechanics of neural tube morphogenesis. *Semin. Cell Dev. Biol.* **130**, 56–69 (2022).

160. van der Spuy, M., Wang, J. X., Kociszewska, D. & White, M. D. The cellular dynamics of neural tube formation. *Biochem. Soc. Trans.* **51**, 343–352 (2023).
161. Nakatsu, T., Uwabe, C. & Shiota, K. Neural tube closure in humans initiates at multiple sites: evidence from human embryos and implications for the pathogenesis of neural tube defects. *Anat. Embryol.* **201**, 455–466 (2000).
162. Knight, G. T. et al. Engineering induction of singular neural rosette emergence within hPSC-derived tissues. *eLife* **7**, e37549 (2018).
163. Britton, G., Heemskerk, I., Hodge, R., Qutub, A. A. & Warmflash, A. A novel self-organizing embryonic stem cell system reveals signaling logic underlying the patterning of human ectoderm. *Development* **146**, dev179093 (2019).
164. Haremaki, T. et al. Self-organizing neuruloids model developmental aspects of Huntington's disease in the ectodermal compartment. *Nat. Biotechnol.* **37**, 1198–1208 (2019).
165. Lee, J.-H. et al. Production of human spinal-cord organoids recapitulating neural-tube morphogenesis. *Nat. Biomed. Eng.* **6**, 435–448 (2022).
166. Fedorova, V. et al. Differentiation of neural rosettes from human pluripotent stem cells in vitro is sequentially regulated on a molecular level and accomplished by the mechanism reminiscent of secondary neurulation. *Stem Cell Res.* **40**, 101563 (2019).
167. Kulesa, P. M. & Fraser, S. E. Cell dynamics during somite boundary formation revealed by time-lapse analysis. *Science* **298**, 991–995 (2002).
168. Sato, Y. & Takahashi, Y. A novel signal induces a segmentation fissure by acting in a ventral-to-dorsal direction in the presomitic mesoderm. *Dev. Biol.* **282**, 183–191 (2005).
169. Marrese, M. et al. In vivo characterization of chick embryo mesoderm by optical coherence tomography-assisted microindentation. *FASEB J.* **34**, 12269–12277 (2020).
170. Nelemans, B. K. A., Schmitz, M., Tahir, H., Merks, R. M. H. & Smit, T. H. Somite division and new boundary formation by mechanical strain. *iScience* **23**, 100976 (2020).
171. Adhyapok, P. et al. A mechanical model of early somite segmentation. *iScience* **24**, 102317 (2021).
172. Sanaki-Matsumiya, M. et al. Periodic formation of epithelial somites from human pluripotent stem cells. *Nat. Commun.* **13**, 2325 (2022).
173. Yaman, Y. I. & Ramanathan, S. Controlling human organoid symmetry breaking reveals signaling gradients drive segmentation clock waves. *Cell* **186**, 513–527.e9 (2023).
174. Miao, Y. et al. Reconstruction and deconstruction of human somitogenesis in vitro. *Nature* **614**, 500–508 (2023).
175. Yamanaka, Y. et al. Reconstituting human somitogenesis in vitro. *Nature* **614**, 509–520 (2023).
176. Liu, Y. et al. A human pluripotent stem cell-based somitogenesis model using microfluidics. *Cell Stem Cell* **31**, 1113–1126.e6 (2024).
177. Gribaudo, S. et al. Self-organizing models of human trunk organogenesis recapitulate spinal cord and spine co-morphogenesis. *Nat. Biotechnol.* **42**, 1243–1253 (2023).
178. Alom Ruiz, S. & Chen, C. S. Microcontact printing: a tool to pattern. *Soft Matter* **3**, 168–177 (2007).
179. Sahni, G., Yuan, J. & Toh, Y. C. Stencil micropatterning of human pluripotent stem cells for probing spatial organization of differentiation fates. *J. Vis. Exp.* **112**, 54097 (2016).
180. Folch, A., Jo, B.-H., Hurtado, O., Beebe, D. J. & Toner, M. Microfabricated elastomeric stencils for micropatterning cell cultures. *J. Biomed. Mater. Res.* **52**, 346–353 (2000).
181. Dillmore, W. S., Yousaf, M. N. & Mrksich, M. A photochemical method for patterning the immobilization of ligands and cells to self-assembled monolayers. *Langmuir* **20**, 7223–7231 (2004).
182. Peterbauer, T., Heitz, J., Olbrich, M. & Hering, S. Simple and versatile methods for the fabrication of arrays of live mammalian cells. *Lab. Chip* **6**, 857–863 (2006).
183. Gumpenberger, T. et al. Adhesion and proliferation of human endothelial cells on photochemically modified polytetrafluoroethylene. *Biomaterials* **24**, 5139–5144 (2003).
184. Aisenbrey, E. A. & Murphy, W. L. Synthetic alternatives to Matrigel. *Nat. Rev. Mater.* **5**, 539–551 (2020).
185. Gjorevski, N. et al. Designer matrices for intestinal stem cell and organoid culture. *Nature* **539**, 560–564 (2016).
186. Cruz-Acuña, R. et al. Synthetic hydrogels for human intestinal organoid generation and colonic wound repair. *Nat. Cell Biol.* **19**, 1326–1335 (2017).
187. Enemchukwu, N. O. et al. Synthetic matrices reveal contributions of ECM biophysical and biochemical properties to epithelial morphogenesis. *J. Cell Biol.* **212**, 113–124 (2015).
188. Blatchley, M. R. & Anseth, K. S. Middle-out methods for spatiotemporal tissue engineering of organoids. *Nat. Rev. Bioeng.* **1**, 329–345 (2023).
189. Yavitt, F. M. et al. In situ modulation of intestinal organoid epithelial curvature through photoinduced viscoelasticity directs crypt morphogenesis. *Sci. Adv.* **9**, eadd5668 (2023).
This article describes a material platform to spatiotemporally modulate hydrogel viscoelasticity through a photo-induced hydrogel cross-link exchange reaction to control crypt morphogenesis in intestinal organoids.
190. Manhas, J., Edelstein, H. I., Leonard, J. N. & Morsut, L. The evolution of synthetic receptor systems. *Nat. Chem. Biol.* **18**, 244–255 (2022).
191. Chen, W. C. W. et al. A synthetic transcription platform for programmable gene expression in mammalian cells. *Nat. Commun.* **13**, 6167 (2022).
192. Toda, S., Blauch, L. R., Tang, S. K. Y., Morsut, L. & Lim, W. A. Programming self-organizing multicellular structures with synthetic cell-cell signaling. *Science* **361**, 156–162 (2018).
193. Jurkowski, T. P., Ravichandran, M. & Stepper, P. Synthetic epigenetics — towards intelligent control of epigenetic states and cell identity. *Clin. Epigenetics* **7**, 18 (2015).
194. Amadei, G. et al. Inducible stem-cell-derived embryos capture mouse morphogenetic events in vitro. *Dev. Cell* **56**, 366–382.e9 (2021).
195. Skylar-Scott, M. A. et al. Orthogonally induced differentiation of stem cells for the programmatic patterning of vascularized organoids and bioprinted tissues. *Nat. Biomed. Eng.* **6**, 449–462 (2022).
196. Duguay, D., Foty, R. A. & Steinberg, M. S. Cadherin-mediated cell adhesion and tissue segregation: qualitative and quantitative determinants. *Dev. Biol.* **253**, 309–323 (2003).
197. Foty, R. A. & Steinberg, M. S. The differential adhesion hypothesis: a direct evaluation. *Dev. Biol.* **278**, 255–263 (2005).
198. Bao, M. et al. Stem cell-derived synthetic embryos self-assemble by exploiting cadherin codes and cortical tension. *Nat. Cell Biol.* **24**, 1341–1349 (2022).
199. Stevens, A. J. et al. Programming multicellular assembly with synthetic cell adhesion molecules. *Nature* **614**, 144–152 (2023).
This article describes a wide array of synthetic cell adhesion molecules by combining orthogonal extracellular interactions with endogenous intracellular domains, which enables programmable assembly of multicellular architectures.
200. Deglincerti, A. et al. Self-organization of the in vitro attached human embryo. *Nature* **533**, 251–254 (2016).
201. Shahbazi, M. N. et al. Self-organization of the human embryo in the absence of maternal tissues. *Nat. Cell Biol.* **18**, 700–708 (2016).
202. Zhai, J. et al. Primate gastrulation and early organogenesis at single-cell resolution. *Nature* **612**, 732–738 (2022).
203. Gong, Y. et al. Ex utero monkey embryogenesis from blastocyst to early organogenesis. *Cell* **186**, 2092–2110.e23 (2023).
204. Xu, Y. et al. A single-cell transcriptome atlas profiles early organogenesis in human embryos. *Nat. Cell Biol.* **25**, 604–615 (2023).
205. Tyser, R. C. V. et al. Single-cell transcriptomic characterization of a gastrulating human embryo. *Nature* **600**, 285–289 (2021).
206. Zeng, B. et al. The single-cell and spatial transcriptional landscape of human gastrulation and early brain development. *Cell Stem Cell* **30**, 851–866.e7 (2023).
207. Meistermann, D. et al. Integrated pseudotime analysis of human pre-implantation embryo single-cell transcriptomes reveals the dynamics of lineage specification. *Cell Stem Cell* **28**, 1625–1640.e6 (2021).
208. Rossant, J. & Fu, J. Why researchers should use human embryo models with caution. *Nature* **622**, 454–456 (2023).
209. Rivron, N. C., Martinez Arias, A., Pera, M. F., Moris, N. & M'hamdi, H. I. An ethical framework for human embryology with embryo models. *Cell* **186**, 3548–3557 (2023).
210. Clark, A. T. et al. Human embryo research, stem cell-derived embryo models and in vitro gametogenesis: considerations leading to the revised ISSCR guidelines. *Stem Cell Rep.* **16**, 1416–1424 (2021).
211. Birtele, M. et al. Non-synaptic function of the autism spectrum disorder-associated gene SYNGAP1 in cortical neurogenesis. *Nat. Neurosci.* **26**, 2090–2103 (2023).
212. Hyun, I., Munsie, M., Pera, M. F., Rivron, N. C. & Rossant, J. Toward guidelines for research on human embryo models formed from stem cells. *Stem Cell Rep.* **14**, 169–174 (2020).
213. Blasimme, A. & Sugarman, J. Human stem cell-derived embryo models: toward ethically appropriate regulations and policies. *Cell Stem Cell* **30**, 1008–1012 (2023).

Acknowledgements

The authors thank M. Yang for invaluable work on illustrations and A. H. Terhune for support in early-stage manuscript editing. Embryo modelling research in the Fu laboratory is supported by the Michigan–Cambridge Collaboration Initiative, University of Michigan Mcubed Fund, University of Michigan Mid-career Biosciences Faculty Achievement Recognition Award, National Science Foundation (PFI-TT 2213845, I-Corps 2112458, CMMI 1917304, CBET 1901718 and CMMI 2325361) and NIH (R21 NS113518, R21 HD100931, R21 HD105126, R21 NS127983, R21 HD109635, R21 HD105192, R33 CA261696, R01 GM134535 and R01 NS129850). The authors apologize to all researchers whose work could not be cited owing to space restrictions.

Author contributions

X.X., Y.L. and J.F. wrote the article. X.X. generated figures. All authors contributed to the conceptualization of the article.

Competing interests

The authors declare no competing interests.

Additional information

Peer review information *Nature Reviews Bioengineering* thanks Jacob Hanna and the other, anonymous, reviewer(s) for their contribution to the peer review of this work.

Publisher's note Springer Nature remains neutral with regard to jurisdictional claims in published maps and institutional affiliations.

Springer Nature or its licensor (e.g. a society or other partner) holds exclusive rights to this article under a publishing agreement with the author(s) or other rightsholder(s); author self-archiving of the accepted manuscript version of this article is solely governed by the terms of such publishing agreement and applicable law.

© Springer Nature Limited 2024